SIAM J. APPL. MATH.
Vol. 72, No. 3, pp. 740–766

STATIONARY SOLUTIONS OF A VOLUME-FILLING CHEMOTAXIS MODEL WITH LOGISTIC GROWTH AND THEIR STABILITY*

MANJUN MA†, CHUNHUA OU‡, AND ZHI-AN WANG§

Abstract. In this paper, we derive the conditions for the existence of stationary solutions (i.e., nonconstant steady states) of a volume-filling chemotaxis model with logistic growth over a bounded domain subject to homogeneous Neumann boundary conditions. At the same time, we show that the same system without the chemotaxis term does not admit pattern formations. Moreover, based on an explicit formula for the stationary solutions, which is derived by asymptotic bifurcation analysis, we establish the stability criteria and find a selection mechanism of the principal wave modes for the stable stationary solution by estimating the leading term of the principal eigenvalue. We show that all bifurcations except the one at the first location of the bifurcation parameter are unstable, and if the pattern is stable, then its principal wave mode must be a positive integer which minimizes the bifurcation parameter. For a special case where the carrying capacity is one half, we find a necessary and sufficient condition for the stability of pattern solutions. Numerical simulations are presented, on the one hand, to illustrate and fit our analytical results and, on the other hand, to demonstrate a variety of interesting spatio-temporal patterns, such as chaotic dynamics and the merging process, which motivate an interesting direction to pursue in the future.

Key words. chemotaxis, volume-filling effect, global-in-time existence, stationary solutions, pattern formation, bifurcation, stability

AMS subject classifications. 35K55, 35K57, 35K45, 35K50, 92C15, 92C17, 92B99

DOI. 10.1137/110843964

1. Introduction.

The process of generation of spontaneous patterns (i.e., self-organization) involves many instances where symmetry is broken or a more symmetric state develops into a less symmetric one. It is striking that many of these breaks in symmetry have no external trigger, but are instigated internally. Hence a natural question arises: how can this process be done? The significant progress toward this question was made in 1952 by Alan Turing, whose paper [29] was considered one of the most influential works in theoretical biology. Turing thought about a simple model with two morphogens (chemical species): a short-range activator and a long-range inhibitor. Both morphogens diffuse in space, but at different rates, and the inhibitor diffuses faster than the activator. The combination of local strong activation and long-range inhibition is able to instigate a spatial patterning process. Turing proposed a mathematical model based on a couple of partial differential equations encapsulating these elements, known as a reaction-diffusion model (see, e.g., [18]). Turing's revolutionary contribution was that passive diffusion could interact with chemical reaction

*Received by the editors August 9, 2011; accepted for publication (in revised form) February 28, 2012; published electronically May 24, 2012.
http://www.siam.org/journals/siap/72-3/84396.html
†Department of Mathematics, College of Sciences, China Jiliang University, Hangzhou, Zhejiang, 310018, China (mmj@cjlu.edu.cn). This author's work was supported by NSF-Y6100166 of Zhejiang province.
‡Department of Mathematics and Statistics, Memorial University of Newfoundland, St. John's, NL, A1C 5S7, Canada (ou@mun.ca). This author's work was supported in part by the NSERC grant of Canada.
§Department of Applied Mathematics, The Hong Kong Polytechnic University, Hung Hom, Kowloon, Hong Kong (mawza@polyu.edu.hk). This author's work was supported by the Mathematical Biosciences Institute (MBI) at The Ohio State University through the National Science Foundation under grant DMS 0931642 and in part by Hong Kong RGC General Research Fund 502711.

and destabilize the homogeneity. This result comes counterintuitively because passive diffusion is a stabilizing force that increases homogeneity in a single equation.

While the Turing pattern is formed passively by diffusion, most biological pattern onset involves an active response to the pattern which contributes to subsequent morphogenesis, where cell movement plays a crucial role, such as slime mold formation by *Dictyostelium discoideum* [11], fish pigmentation [24], gastrulation and limb development in the chick embryo [17, 34], various aggregation of bacteria [3, 4], primitive streak formation [25], and so on. The trigger for such movement is chemotaxis, a process by which cells change their state of movement in response to the presence of a chemical concentration gradient, approaching chemically favorable environments and avoiding unfavorable ones. Chemotaxis is a leading mechanism accounting for morphogenesis and self-organization of various biological coherent and enthralled structures, such as aggregates, fruiting bodies, clusters, spirals, spots, rings, labyrinthine patterns, and stripes, which have been observed in experiments [3, 4, 8, 7, 18]. Keller and Segel [14, 15] proposed the first mathematical model for describing the aggregation phase of *Dictyostelium discoideum*, and since then a vast number of results [12, 10] have been developed for the Keller–Segel-type model.

The purpose of this paper is to study the existence and stability of stationary solutions (i.e., nonconstant steady states) of a volume-filling chemotaxis model with logistic cell growth proposed by Painter and Hillen [22]:

$$\begin{cases} \dfrac{\partial u}{\partial t} = \nabla \cdot (d_1 \nabla u - \chi u(1-u)\nabla v) + \mu u(1-u/u_c), \\ \dfrac{\partial v}{\partial t} = d_2 \Delta v + \alpha u - \beta v, \end{cases} \tag{1.1}$$

where $(x,t) \in \Omega \times [0,+\infty)$ and Ω is a bounded domain in $\mathbb{R}^N$ with smooth boundary $\partial\Omega$. $u(x,t)$ is the cell density and $v(x,t)$ denotes the chemical concentration, and $d_1 > 0$ and $d_2 > 0$ denote the cell and chemical diffusion coefficients, respectively. $\chi > 0$ is referred to as the chemosensitivity (or chemotactic coefficient) measuring the strength of the chemotactic response. The term $u(1-u)\nabla v$ represents the chemotactic flux under a volume constraint 1 (called crowding capacity), meaning that the chemotactic movement will be suppressed at the aggregation location where the cell density reaches the crowding capacity 1. The term $\mu u(1-u/u_c)$ describes the logistic growth of cells with growth rate $\mu > 0$ and carrying capacity u_c fulfilling $0 < u_c \leq 1$. The term $\alpha u - \beta v$ asserts that the chemical has a linear production and degradation, where $\alpha, \beta > 0$, and the term αu essentially implies that the chemical is secreted by cells themselves and the resulting pattern formation will be a process of self-organization.

We shall consider the system (1.1) subject to initial data

$$u(x,0) = u_0(x) \geq 0, \quad v(x,0) = v_0(x) \geq 0, \quad x \in \Omega, \tag{1.2}$$

and Neumann boundary conditions

$$\frac{\partial u}{\partial \nu} = \frac{\partial v}{\partial \nu} = 0 \quad \text{on} \quad \partial\Omega \quad \text{for} \quad t > 0, \tag{1.3}$$

with ν denoting the outward unit normal vector on $\partial\Omega$.

The chemotaxis models with logistic growth but without a volume-filling effect have been studied in [20, 28, 31]. The stationary solutions of the volume-filling chemotaxis model without a growth term (i.e., $\mu = 0$) have been obtained in [16, 33, 13, 26].

Although the global attractor and traveling wave solutions of (1.1) with $\mu > 0$ have been obtained in [32, 21], respectively, the stationary solutions have not been studied as far as we know. The present paper will be focused on the study of the stationary solutions of the volume-filling chemotaxis model (1.1) with $\mu > 0$. The main results are threefold: (i) Applying the index theory [1, 5], we derive the sufficient conditions for the existence of stationary solutions of (1.1) with homogeneous Neumann boundary conditions. It turns out that these conditions are closely related to the linear stability conditions for pattern formations. In the derivation, we also show that the positive constant steady state of the system without the chemotaxis term is globally asymptotically stable. The nonconstant steady states arise only when chemotaxis sets in. All results in this part are proved rigorously. (ii) By deriving an explicit formula for the stationary solutions from the asymptotic bifurcation analysis and performing the stability analysis in estimating the leading terms of principal eigenvalues, we find a stability criterion which also provides a selection mechanism for the principal wave modes of the stable stationary pattern solutions of system (1.1)–(1.3). All results in this part are derived by formal asymptotic analysis. (iii) By showing numerical simulations, we employ our theoretical results to interpret the underlying mechanism of various patterns and raise numerous interesting questions for future study.

The rest of this paper is arranged as follows. In section 2, we present some preliminary results for the model. The existence of stationary solutions via the degree index method is established in section 3. A comparative study of linear stability analysis for pattern formations is implemented in section 4. In section 5, we first derive a formula for the pattern solutions via asymptotic bifurcation analysis and then find the stability/instability conditions for the stationary solutions by estimating the principal eigenvalues explicitly. In a special case when $u_c = \frac{1}{2}$, a necessary and sufficient stability condition is given. In section 6, numerical simulations are performed to interpret the pattern formations in terms of our analytical results. The significance of current studies is outlined and some further works are presented in section 7.

2. Preliminary results.

Notation. Throughout this paper, let $W^{m,p}(\Omega, \mathbb{R}^N)$ $(m \geq 1,\ 1 < p < +\infty)$ be the Sobolev space of $\mathbb{R}^N$-valued functions with norm $\|\cdot\|_{m,p}$. When $p = 2$, $W^{m,2}(\Omega, \mathbb{R}^N)$ is written as $H^m(\Omega)$. Let $L^p(\Omega)$ $(1 \leq p \leq \infty)$ denote the usual Lebesgue space in a bounded domain $\Omega \subset \mathbb{R}^N$ with norm $\|f\|_{L^p} = (\int_\Omega |f(x)|^p dx)^{1/p}$ for $1 \leq p < \infty$ and $\|f\|_{L^\infty} = \operatorname{ess\,sup}_{x\in\Omega} |f(x)|$. When $p \in (N, +\infty)$, $W^{1,p}(\Omega, \mathbb{R}^2) \hookrightarrow C(\Omega, \mathbb{R}^2)$, whose norm is denoted by $\|\cdot\|$.

From now on we fix $p > N$ and define

$$W = \left\{ \omega = (u, v) \in W^{1,p}(\Omega, \mathbb{R}^2) \,\middle|\, \frac{\partial \omega}{\partial \nu}\Big|_{\partial\Omega} = 0 \right\}.$$

The existence of global bounded classical solutions of (1.1)–(1.3) has been established in [30] by the maximum principle and Amann's theory [2]. For convenience, we cite the results in the following lemma.

LEMMA 2.1. *Let $\omega_0 = (u_0, v_0) \in W$ with $0 \leq u_0 \leq 1,\ 0 \leq v_0 \leq \frac{\alpha}{\beta}$ on $\overline{\Omega}$. Then the initial-boundary value problem* (1.1)–(1.3) *possesses a unique classical solution (u, v) satisfying the following:*

(i) $(u, v) \in C([0, +\infty); W) \cap C^{2,1}(\overline{\Omega} \times (0, +\infty); \mathbb{R}^2)$;

(ii) $0 \leq u \leq 1,\ 0 \leq v \leq \frac{\alpha}{\beta}$ *for any* $(x, t) \in \overline{\Omega} \times [0, +\infty)$;

(iii) *the solution semigroup* $\Pi(t; \omega_0)$ *generates a semidynamical system on* W.

To show that the pattern formation of system (1.1)–(1.3) is driven by the chemotaxis, we first discuss the dynamics of the corresponding system of ordinary differential equations

$$\begin{cases} \frac{du}{dt} = \mu u(1 - \frac{u}{u_c}), \\ \frac{dv}{dt} = \alpha u - \beta v, \\ u(0) = u^0, \quad v(0) = v^0 \end{cases} \tag{2.1}$$

and the corresponding reaction-diffusion equations in the absence of the chemotaxis term

$$\begin{cases} \frac{\partial u}{\partial t} = d_1 \triangle u + \mu u(1 - \frac{u}{u_c}), \ x \in \Omega, \ t > 0, \\ \frac{\partial v}{\partial t} = d_2 \Delta v + \alpha u - \beta v, \ x \in \Omega, \ t > 0, \\ \frac{\partial u}{\partial \nu} = \frac{\partial v}{\partial \nu} = 0, \ x \in \partial\Omega, \ t > 0, \\ u(x,0) = u_0(x) \geq 0, \ v(x,0) = v_0(x) \geq 0, \ x \in \Omega. \end{cases} \tag{2.2}$$

Evidently, (2.1) has two equilibria: the zero equilibrium $\mathbf{0} = (0,0)$ and the positive equilibrium $\widetilde{\omega} = (\widetilde{u}, \widetilde{v}) = (u_c, \frac{\alpha}{\beta} u_c)$. The following two propositions will show that Turing patterns cannot emerge from the system (2.2).

PROPOSITION 2.2. *The positive equilibrium* $(\widetilde{u}, \widetilde{v}) = (u_c, \frac{\alpha}{\beta} u_c)$ *of* (2.1) *is globally asymptotically stable.*

This result is trivial. So we omit its proof.

Let $0 = \lambda_1 < \lambda_2 < \lambda_3 < \cdots$ be the eigenvalues of the operator $-\Delta$ on Ω with the homogeneous Neumann boundary condition, let $E(\lambda_i)$ be the eigenspace corresponding to λ_i in $H^1(\Omega, \mathbb{R}^2)$, let $\{\varphi_{ij} : j = 1, \ldots, \dim E(\lambda_i)\}$ be an orthonormal basis of $E(\lambda_i)$, and let $X_{ij} = \{\mathbf{c}\varphi_{ij} : \mathbf{c} \in \mathbb{R}^2\}$. Let $X = H^1(\Omega, \mathbb{R}^2)$. Then we have

$$X_i = \bigoplus_{j=1}^{\dim E(\lambda_i)} X_{ij}, \qquad X = \bigoplus_{i=1}^{\infty} X_i. \tag{2.3}$$

PROPOSITION 2.3. *The positive constant steady state* $(u_c, \frac{\alpha}{\beta} u_c)$ *of system* (2.2) *is globally asymptotically stable. Consequently, system* (2.2) *does not have nonconstant steady states.*

Proof. System (2.2) can be rewritten as

$$\frac{\partial \omega}{\partial t} = \mathcal{D}\Delta\omega + \mathbb{F}(\omega), \tag{2.4}$$

where $\mathcal{D}$ and $\mathbb{F}(\omega)$ are defined as

$$\mathcal{D} = \begin{pmatrix} d_1 & 0 \\ 0 & d_2 \end{pmatrix}, \qquad \mathbb{F}(\omega) = \begin{pmatrix} \mu u(1 - u/u_c) \\ \alpha u - \beta v \end{pmatrix}. \tag{2.5}$$

The linearized system of (2.4) at $\widetilde{\omega}$ is

$$\frac{\partial \omega}{\partial t} = \mathcal{L}\omega$$

with $\mathcal{L} = \mathcal{D}\Delta + \mathbb{F}_\omega(\widetilde{\omega})$. Under the operator $\mathcal{L}$, the subspace X_i is invariant for each $i \geq 1$, and η is an eigenvalue of $\mathcal{L}$ if and only if it is an eigenvalue of the matrix

$-\lambda_i\mathcal{D}+\mathbb{F}_\omega(\widetilde{\omega})$ for some $i \geq 1$, and its corresponding eigenvector is in X_i. By a simple computation, the characteristic polynomial of the matrix $-\lambda_i\mathcal{D}+\mathbb{F}_\omega(\widetilde{\omega})$ is

$$\mathcal{P}_i(\eta) = (\eta+\mu+\lambda_i d_1)(\eta+\beta+\lambda_i d_2), \qquad i \geq 1,$$

and the two roots $\eta_{i,1},\ \eta_{i,2}$ of $\mathcal{P}_i(\eta)=0$ satisfy

$$\eta_{i,1},\ \eta_{i,2} \leq \max\{-\mu,-\beta\} < 0.$$

Hence $(u_c, \frac{\alpha}{\beta}u_c)$ is locally stable. Since the reaction terms in system (2.2) are Lipschitz, (2.2) generates a semiflow on $C(\bar{\Omega},\mathbb{R}^2)$ which is strongly monotone with respect to the cone $C_+(\bar{\Omega},\mathbb{R}^2) = \{(u,v) \in C(\bar{\Omega},\mathbb{R}^2) | u > 0, v > 0\}$ (see [27]), and then $(u_c, \frac{\alpha}{\beta}u_c)$ is globally attractive. Hence, $(u_c, \frac{\alpha}{\beta}u_c)$ is globally asymptotically stable. The proof is complete. ∎

3. Stationary solutions of chemotaxis system (1.1)–(1.3). In this section, we will verify that the volume-filling chemotaxis system (1.1)–(1.3) has nonconstant steady states (i.e., stationary patterns) under appropriate conditions.

To show the existence of stationary patterns, we consider the steady state problem of (1.1)–(1.3):

$$\begin{cases} -\nabla\cdot(d_1\nabla u - \chi u(1-u)\nabla v) = \mu u(1-u/u_c), & x\in\Omega,\\ -d_2\Delta v = \alpha u - \beta v, & x\in\Omega,\\ \frac{\partial u}{\partial\nu} = \frac{\partial v}{\partial\nu} = 0, & x\in\partial\Omega. \end{cases} \tag{3.1}$$

The lemma below shows that the positive solutions of (3.1) are uniformly bounded.

LEMMA 3.1. *Let (u,v) be a nonnegative (classical) solution to the boundary value problem of elliptic system* (3.1). *Then*

$$0 \leq u \leq 1,\ 0 \leq v \leq \frac{\alpha}{\beta} \quad \textit{for all} \quad x \in \overline{\Omega}. \tag{3.2}$$

Proof. Define differential operator $L : \mathbb{R} \longrightarrow \mathbb{R}$ as

$$Lu = -d_1\Delta u + \chi(1-u)\nabla u\nabla v - \chi u\nabla u\nabla v + \chi u(1-u)\Delta v$$

and function $f(u) = \mu u(1-u/u_c)$. Then the first equation of (3.1) can be written as $Lu = f(u)$ for $x\in\Omega$ with boundary condition $\frac{\partial u}{\partial\nu}=0$. Let $\bar{u}=1$. Noting that $u_c \leq 1$, we have

$$0 = L\bar{u} \geq f(\bar{u}), \qquad x\in\Omega,$$

which, together with boundary condition $\frac{\partial\bar{u}}{\partial\nu}=0$ for $x\in\partial\Omega$, indicates that $\bar{u}=1$ is a supersolution of the equation $Lu=f(u)$ for all $x\in\overline{\Omega}$. Noticing that f is smooth, by comparison principle, we have $0\leq u\leq\bar{u}=1$ for all $x\in\overline{\Omega}$ by taking into account that u is nonnegative. Similarly, if we define $Kv=-d_2\Delta v$ and $g(u,v)=\alpha u-\beta v$, we can verify that $0=K\bar{v}\geq g(u,\bar{v})$ in $x\in\Omega$ for all $0\leq u\leq 1$, where $\bar{v}=\frac{\alpha}{\beta}$. Noticing that $\frac{\partial\bar{v}}{\partial\nu}=0$ for $x\in\partial\Omega$, $\bar{v}$ is a supersolution of $Kv=g(u,v)$ and the proof is then completed by comparison principle. ∎

By choosing $\underline{k} > \frac{1-u_c}{u_c}\mu$ and $\overline{k} > \beta$, system (3.1) can be rewritten as

$$\begin{cases} -\nabla\cdot(d_1\nabla u - \chi u(1-u)\nabla v) + \underline{k}u = \underline{k}u + \mu u(1-u/u_c), & x\in\Omega,\\ -d_2\Delta v + \overline{k}v = \alpha u + (\overline{k}-\beta)v, & x\in\Omega,\\ \frac{\partial u}{\partial\nu} = \frac{\partial v}{\partial\nu} = 0, & x\in\partial\Omega. \end{cases} \tag{3.3}$$

In terms of this setting, we proceed to set up a fixed point equation in the positive cone

$$\mathbb{P}_+ = \left\{ (u,v) \in C(\overline{\Omega};\mathbb{R}^2) \mid 0 \le u \le 1, 0 \le v \le \frac{\alpha}{\beta} \right\}$$

of the Banach space $\mathbb{P} = C(\overline{\Omega};\mathbb{R}^2)$ and use the fixed point index technique to obtain the existence of nonconstant steady states of (3.1).

For given $\psi = (\psi_1, \psi_2)$ in $\mathbb{P}_+$, we define $\omega = \Psi(\psi)$ to be the solution of the system

$$\begin{cases} -\nabla \cdot (d_1 \nabla u - \chi u(1-u)\nabla v) + \underline{k} u = \underline{k}\psi_1 + \mu\psi_1(1-\psi_1/u_c), & x \in \Omega, \\ -d_2 \Delta v + \overline{k} v = \alpha\psi_1 + (\overline{k} - \beta)\psi_2, & x \in \Omega, \\ \frac{\partial u}{\partial \nu} = \frac{\partial v}{\partial \nu} = 0, & x \in \partial\Omega. \end{cases} \tag{3.4}$$

Then we have the following lemma.

LEMMA 3.2. *$\Psi : \mathbb{P}_+ \to \mathbb{P}_+$ is a well-defined completely continuous operator. Moreover, the fixed points of Ψ in $\mathbb{P}_+$ are solutions of* (3.1).

Proof. It is easy to see that the second equation of (3.4) has a unique solution $v \in C^2(\Omega)$ (see [9, Theorem 6.31]). Substituting the result into the equation for u and using the properties of quasi-linear equations of parabolic type with Neumann boundary value conditions, we can obtain a unique $u \in C^2(\Omega)$ from the first equation of (3.4). Hence, Ψ is a well-defined map.

System (3.4) can be rewritten in the matrix form

$$\begin{cases} -\nabla \cdot (\mathbb{A}(\omega)\nabla\omega) + \mathbb{D} \cdot \omega = \mathbb{G}(\psi), & x \in \Omega, \\ \frac{\partial \omega}{\partial \nu} = 0, & x \in \partial\Omega, \end{cases} \tag{3.5}$$

where

$$\mathbb{A}(\omega) = \begin{pmatrix} d_1 & -\chi u(1-u) \\ 0 & d_2 \end{pmatrix}, \ \mathbb{D} = \begin{pmatrix} \underline{k} & 0 \\ 0 & \overline{k} \end{pmatrix}, \ \mathbb{G}(\psi) = \begin{pmatrix} \underline{k}\psi_1 + \mu\psi_1(1-\psi_1/u_c) \\ \alpha\psi_1 + (\overline{k} - \beta)\psi_2 \end{pmatrix}.$$

Since $\mathbb{A}(\omega)$ and $\mathbb{D}$ are positive definite and $\mathbb{G}(\psi) \ge 0$ in $\mathbb{P}_+$, Ψ maps $\mathbb{P}_+$ into itself.

Using the same arguments of Lemma 3.1 in [6], we can derive the complete continuity of Ψ. The proof is then finished. ∎

The map Ψ can be expressed as

$$\Psi = \Gamma \circ \mathbb{G} \tag{3.6}$$

with Γ being the inverse operator of $-\nabla \cdot (\mathbb{A} \circ \nabla) + \mathbb{D}$.

System (3.1) is now equivalent to the fixed point problem on $\mathbb{P}_+$:

$$\omega = \Psi(\omega) = \Gamma \circ \mathbb{G}(\omega), \qquad \omega \in \mathbb{P}_+. \tag{3.7}$$

It is trivial to check that $\mathbf{0} = (0,0)$ and $\widetilde{\omega} = (u_c, \frac{\alpha}{\beta}u_c)$ are constant fixed points of Ψ. Our purpose is to find the nonconstant fixed points of Ψ in $\mathbb{P}_+$ by the degree index method. Therefore, we need to compute the degree indices of the two fixed points $\mathbf{0}$ and $\widetilde{\omega}$ and use them to derive the existence of the nonconstant fixed points.

Let $\Psi'_+(\mathbf{0})$ denote the derivative of $\Psi(\omega)$ at $\omega = (0,0)$ in the direction of the cone $\mathbb{P}_+$. Then

$$\Psi'_+(\mathbf{0}) = K \circ G,$$

where

$$K = \begin{pmatrix} (-d_1\Delta + \underline{k})^{-1} & 0 \\ 0 & (-d_2\Delta + \overline{k})^{-1} \end{pmatrix}, \qquad G = \begin{pmatrix} \underline{k} + \mu & 0 \\ \alpha & \overline{k} - \beta \end{pmatrix}.$$

Observe that K is a compact, positive linear operator on $\mathbb{P}_+$, together with the boundary condition in (3.5). G is also a compact, positive linear operator on $\mathbb{P}_+$ and $G(\mathbf{0}) = \mathbf{0}$. Therefore, $\Psi'_+(\mathbf{0}) : \mathbb{P}_+ \to \mathbb{P}_+$ is a positive, compact linear operator. The lemma below can be obtained through a simple computation.

LEMMA 3.3. *The eigenvalue problem $\Psi'_+(\mathbf{0})\psi = \sigma\psi$ with $\psi = (\psi_1, \psi_2)$ is equivalent to*

$$\begin{cases} -d_1\Delta\psi_1 + \underline{k}\psi_1 = \frac{1}{\sigma}(\underline{k} + \mu)\psi_1, & x \in \Omega, \\ -d_2\Delta\psi_2 + \overline{k}\psi_2 = \frac{1}{\sigma}(\alpha\psi_1 + (\overline{k} - \beta)\psi_2), & x \in \Omega, \\ \frac{\partial\psi_1}{\partial\nu} = \frac{\partial\psi_2}{\partial\nu} = 0, & x \in \partial\Omega. \end{cases} \tag{3.8}$$

System (3.8) can be rewritten as

$$\begin{cases} -\nabla \cdot (\mathcal{D}\nabla\psi) + \mathbb{D} \cdot \psi = \sigma^{-1} g(\psi), & x \in \Omega, \\ \frac{\partial\psi}{\partial\nu} = 0, & x \in \partial\Omega, \end{cases} \tag{3.9}$$

where

$$g(\psi) = \begin{pmatrix} (\underline{k} + \mu)\psi_1 \\ \alpha\psi_1 + (\overline{k} - \beta)\psi_2 \end{pmatrix}.$$

Since $\Psi'_+(\mathbf{0})$ is positive and compact, there is only one positive eigenfunction to (3.9) corresponding to the largest eigenvalue. Then an assertion on the eigenvalue problem of $\Psi'_+(\mathbf{0})$ can be made.

LEMMA 3.4. *Assume that $\lambda_i \neq \frac{\mu}{d_1}$ for all $i \geq 1$. Then 1 is not an eigenvalue of $\Psi'_+(\mathbf{0})$ corresponding to an eigenvector in $\mathbb{P}_+$ and $\Psi'_+(\mathbf{0})$ has an eigenvalue larger than 1 with a corresponding eigenvector in $\mathbb{P}_+$, that is,* $\operatorname{index}(\Psi, \mathbf{0}) = 0$.

Proof. The eigenvalue problem (3.8) can also be rewritten as

$$\begin{pmatrix} -d_1\Delta + \underline{k} - (\underline{k} + \mu)/\sigma & 0 \\ -\alpha/\sigma & -d_2\Delta + \overline{k} - (\overline{k} - \beta)/\sigma \end{pmatrix} \psi = 0, \tag{3.10}$$

which is equivalent to

$$\begin{pmatrix} \lambda_i d_1 + \underline{k} - (\underline{k} + \mu)/\sigma & 0 \\ -\alpha/\sigma & \lambda_i d_2 + \overline{k} - (\overline{k} - \beta)/\sigma \end{pmatrix} \psi = 0, \qquad i \geq 1. \tag{3.11}$$

Since $\lambda_i \neq \frac{\mu}{d_1}$ for all $i \geq 1$, it is clear that 1 is not an eigenvalue of $\Psi'_+(\mathbf{0})$ with an eigenvector in $\mathbb{P}_+$. On the other hand, when $\lambda_1 = 0$, there exists an eigenvalue $\sigma = 1 + \frac{\mu}{\underline{k}} > 1$, and (3.11) is equivalent to

$$\psi_1 = \frac{1}{\alpha}((\sigma - 1)\overline{k} + \beta)\psi_2, \tag{3.12}$$

which has a positive solution. Hence $\Psi'_+(\mathbf{0})$ possesses a positive eigenvalue $\sigma > 1$ with a positive eigenvector. The proof is complete. ∎

The following lemma is about the boundedness of the fixed point, which is a direct consequence of Lemma 3.1.

LEMMA 3.5. *There exists a constant* $R > \widetilde{R} = \max\{1, \frac{\alpha}{\beta}\}$ *such that*

$$\Psi(\omega) = \varrho\omega, \qquad \varrho \geq 1, \tag{3.13}$$

has no solution $\omega \in \mathbb{P}_+$ *satisfying* $\|\omega\| = R$.

Lemmas 3.4–3.5 allow us to apply [1, Lemma 13.1 and Theorem 13.2(i)] to make a conclusion.

LEMMA 3.6. *For any* $r > 0$, *let* $P_r = \{\omega \in \mathbb{P}_+ : \|\omega\| < r\}$. *If* $\lambda_i \neq \frac{\mu}{d_1}$, $i \geq 1$, *then there exists* r_0 *such that* $0 < r_0 < R$ *and for any* $r \in (0, r_0]$,

$$\operatorname{index}(\Psi, P_R \backslash \overline{P_r}) = +1.$$

In particular, there is a fixed point of Ψ *in* $P_R \backslash \overline{P_r}$, *where* R *is as in Lemma* 3.5.

Now we need to calculate the index of the constant fixed point $\widetilde{\omega}$ of Ψ in $P_R \backslash \overline{P_r}$ to verify the existence of a nonconstant positive fixed point of Ψ. Let

$$\mathbb{J} = I - \Psi = I - \Gamma \circ \mathbb{G}. \tag{3.14}$$

Then the fixed point of the operator Ψ is just the zero point of the operator $\mathbb{J}$. The converse is also true.

Recall that if $D_\omega \mathbb{J}(\widetilde{\omega})$ is invertible, the index of $\mathbb{J}$ at the zero point $\widetilde{\omega}$ is defined as

$$\operatorname{index}(\mathbb{J}, \widetilde{\omega}) = (-1)^\gamma,$$

where γ is the sum of the algebraic multiplicities of the negative eigenvalues of $D_\omega \mathbb{J}(\widetilde{\omega})$ (see Theorem 2.8.1 in [19]). From [1, Theorem 11.4], we can derive the relation between $\operatorname{index}(\Psi, \widetilde{\omega})$ and $\operatorname{index}(\mathbb{J}, \widetilde{\omega})$.

LEMMA 3.7. *If* $\widetilde{\omega}$ *is an isolated fixed point of* Ψ, *then both the index of the operator* Ψ *at the fixed point* $\widetilde{\omega}$ *and the index of the operator* $\mathbb{J}$ *at its zero point* $\widetilde{\omega}$ *are well-defined and satisfy*

$$\operatorname{index}(\Psi, \widetilde{\omega}) = \operatorname{index}(\mathbb{J}, \widetilde{\omega}).$$

By (3.3), (3.7), and (3.14), we obtain

$$\begin{aligned} D_\omega \mathbb{J}(\widetilde{\omega}) &= I - D_\omega(\Gamma \circ \mathbb{G})(\widetilde{\omega}) = I - \Gamma_\omega(\widetilde{\omega}) \circ \mathbb{G}_\omega(\widetilde{\omega}) \\ &= I - (-\nabla \cdot (\mathbb{A}_\omega(\widetilde{\omega}) \circ \nabla) + \mathcal{D})^{-1} \circ \mathbb{G}_\omega(\widetilde{\omega}) \\ &= I - \begin{pmatrix} -d_1\Delta + \underline{k} & \chi u_c(1-u_c)\Delta \\ 0 & -d_2\Delta + \overline{k} \end{pmatrix}^{-1} \begin{pmatrix} \underline{k} - \mu & 0 \\ \alpha & \overline{k} - \beta \end{pmatrix}. \end{aligned} \tag{3.15}$$

We shall use the decomposition (2.3) to analyze the eigenvalues of $D_\omega \mathbb{J}(\widetilde{\omega})$. It is well known that, for each integer $i \geq 1$ and $1 \leq j \leq \dim E(\lambda_i)$, X_{ij} is invariant under $D_\omega \mathbb{J}(\widetilde{\omega})$. Furthermore, the right-hand side of (3.15) can be rewritten as

$$\begin{pmatrix} -d_1\Delta + \underline{k} & \chi u_c(1-u_c)\Delta \\ 0 & -d_2\Delta + \overline{k} \end{pmatrix}^{-1} \begin{pmatrix} -d_1\Delta + \mu & \chi u_c(1-u_c)\Delta \\ -\alpha & -d_2\Delta + \beta \end{pmatrix}.$$

Thus, we have that τ is an eigenvalue of $D_u\mathbb{J}(\widetilde{\omega})$ on X_{ij} if and only if, for some $i \geq 1$, it is an eigenvalue of the matrix

$$M_i \overset{def}{=} \begin{pmatrix} d_1\lambda_i + \underline{k} & -\lambda_i\chi u_c(1-u_c) \\ 0 & d_2\lambda_i + \overline{k} \end{pmatrix}^{-1} \begin{pmatrix} d_1\lambda_i + \mu & -\lambda_i\chi u_c(1-u_c) \\ -\alpha & d_2\lambda_i + \beta \end{pmatrix}.$$

Moreover, $D_\omega\mathbb{J}(\widetilde{\omega})$ is invertible if and only if the matrix M_i is nonsingular for all $i \geq 1$. In terms of this property, we have the following formula:

$$\gamma(D_\omega\mathbb{J}(\widetilde{\omega})) = \sum_{i=1}^{\infty} \dim E(\lambda_i) \times \gamma(M_i), \tag{3.16}$$

where $\gamma(D_\omega\mathbb{J}(\widetilde{\omega}))$ and $\gamma(M_i)$ are the sums of the algebraic multiplicities of the negative eigenvalues of $D_\omega\mathbb{J}(\widetilde{\omega})$ and M_i, respectively. The right-hand side of (3.16) is well-defined, since when i is sufficiently large, λ_i is also sufficiently large and a direct computation of eigenvalues of M_i shows that $\gamma(M_i) = 0$ when $i \geq i_0$ for some large enough positive integer i_0. Usually, to compute $\gamma(M_i)$, we need to use the values of $\det(M_i)$ and $\mathrm{trace}(M_i)$. As such, we first define a function $H(\lambda)$ as follows:

$$\begin{aligned} H(\lambda) &= H(\widetilde{\omega}, \lambda) \\ &= \det \begin{pmatrix} d_1\lambda + \underline{k} & -\lambda\chi u_c(1-u_c) \\ 0 & d_2\lambda + \overline{k} \end{pmatrix}^{-1} \det \begin{pmatrix} d_1\lambda + \mu & -\lambda\chi u_c(1-u_c) \\ -\alpha & d_2\lambda + \beta \end{pmatrix} \end{aligned} \tag{3.17}$$

so that $H(\lambda_i) = \det(M_i)$. Observe that if $H(\lambda_i) \neq 0$, then the number of negative eigenvalues (counting algebraic multiplicity) of M_i is 1 if and only if $H(\lambda_i) < 0$. When $H(\lambda_i) > 0$, $\gamma(M_i)$ is either 0 or 2. Thus, it follows from (3.16) that

$$\gamma(D_\omega\mathbb{J}(\widetilde{\omega})) = \sum_{i\geq 1, H(\lambda_i)<0} \dim E(\lambda_i) \pmod 2.$$

As such, we have the following lemma.

LEMMA 3.8. *Suppose that $H(\lambda_i) \neq 0$ for all $i \geq 1$. Then*

$$\mathrm{index}(\mathbb{J}, \widetilde{\omega}) = (-1)^\gamma, \quad \textit{where} \quad \gamma = \sum_{i\geq 1, H(\lambda_i)<0} \dim E(\lambda_i).$$

Now we need to analyze the sign of $H(\lambda_i)$ to compute γ in the above formula. Since the first factor of $H(\lambda_i)$ is positive, we need only determine the sign of the second factor, which is denoted as

$$h(\lambda) = \det \begin{pmatrix} d_1\lambda + \mu & -\lambda\chi u_c(1-u_c) \\ -\alpha & d_2\lambda + \beta \end{pmatrix}.$$

Through a direct computation we have

$$h(\lambda) = d_1d_2\left\{\lambda^2 + \left[\frac{\mu}{d_1} + \frac{\beta}{d_2} - \frac{\alpha\chi}{d_1d_2}u_c(1-u_c)\right]\lambda + \frac{\mu\beta}{d_1d_2}\right\}. \tag{3.18}$$

In order to have $h(\lambda) < 0$, we require that the discriminant of the quadratic function in (3.18) be positive, that is,

$$\Delta = \left[\frac{\mu}{d_1} + \frac{\beta}{d_2} - \frac{\alpha\chi}{d_1d_2}u_c(1-u_c)\right]^2 - \frac{4\mu\beta}{d_1d_2} > 0.$$

As this paper aims to study the existence of stationary patterns with respect to the chemotactic sensitivity, we will focus on the dependence of $H(\lambda_i)$ on the sensitivity factor χ. Then through a simple computation and analysis we obtain that when

$$\chi > \chi_c = \frac{\mu d_2 + \beta d_1 + 2\sqrt{\mu\beta d_1 d_2}}{\alpha u_c(1-u_c)}, \tag{3.19}$$

equation $h(\lambda) = 0$ has two positive roots $\overline{\lambda_1}(\chi)$, $\overline{\lambda_2}(\chi)$ satisfying $\overline{\lambda_2}(\chi) > \overline{\lambda_1}(\chi) > 0$, where

$$\overline{\lambda_1}(\chi) = \frac{1}{2d_1d_2}\Big(-\eta - \sqrt{\eta^2 - 4d_1d_2\mu\beta}\Big), \qquad \overline{\lambda_2}(\chi) = \frac{1}{2d_1d_2}\Big(-\eta + \sqrt{\eta^2 - 4d_1d_2\mu\beta}\Big) \tag{3.20}$$

and

$$\eta = d_2\mu + d_1\beta - \alpha\chi u_c(1-u_c) < 0.$$

Moreover, we have

$$\begin{cases} H(\lambda) > 0, & \lambda \in (-\infty, \overline{\lambda_1}(\chi)) \cup (\overline{\lambda_2}(\chi), +\infty), \\ H(\lambda) < 0, & \lambda \in (\overline{\lambda_1}(\chi), \overline{\lambda_2}(\chi)). \end{cases} \tag{3.21}$$

Thus, we have the result below.

LEMMA 3.9. *Let d_1, d_2, μ, β, α, and u_c be fixed parameters. Assume that χ is large such that* (3.19) *holds. If there exist integers n_1, n satisfying $n > n_1 \geq 1$ such that*

$$\overline{\lambda_1}(\chi) \in (\lambda_{n_1}, \lambda_{n_1+1}), \qquad \overline{\lambda_2}(\chi) \in (\lambda_n, \lambda_{n+1}) \tag{3.22}$$

and

$$\sum_{i=n_1+1}^{n} \dim E(\lambda_i) \quad \textit{is} \quad \textit{odd}, \tag{3.23}$$

then

$$\operatorname{index}(\mathbb{J}, \widetilde{\omega}) = -1. \tag{3.24}$$

Proof. Recalling the definition of λ_i in section 2 and (3.22), we have

$$\begin{cases} \lambda_i < \overline{\lambda_1}(\chi), & 1 \leq i \leq n_1, \\ \overline{\lambda_1}(\chi) < \lambda_i < \overline{\lambda_2}(\chi), & n_1 + 1 \leq i \leq n, \\ \lambda_i > \overline{\lambda_2}(\chi), & i \geq n+1. \end{cases} \tag{3.25}$$

Then, from (3.21), it follows that

$$\begin{cases} H(\lambda_i) > 0, & 1 \leq i \leq n_1, \\ H(\lambda_i) < 0, & n_1 + 1 \leq i \leq n, \\ H(\lambda_i) > 0, & i \geq n+1. \end{cases} \tag{3.26}$$

Therefore, zero is not an eigenvalue of the matrix M_i for all $i \geq 1$. Then Lemma 3.8 and (3.23) lead to the desired result. ∎

We are now in position to present the main result of this section.

THEOREM 3.10. *Let λ_i, $i \geq 1$, be eigenvalues of the Laplace operator $-\Delta$ under the homogeneous Neumann boundary condition. Then system* (3.1) *has at least one nonconstant positive solution if the following conditions are fulfilled:*

(i) *parameters $d_1,\ d_2,\ \mu,\ \beta,\ \alpha,\ u_c$, and χ satisfy* (3.19)*;*

(ii) *there exist integers $n_1,\ n$ satisfying $n > n_1 \geq 1$ such that $\overline{\lambda_1}(\chi) \in (\lambda_{n_1}, \lambda_{n_1+1})$, $\overline{\lambda_2}(\chi) \in (\lambda_n, \lambda_{n+1})$;*

(iii) *$\lambda_i \neq \frac{\mu}{d_1},\ i \geq 1$;*

(iv) *$\sum_{i=n_1+1}^{n} \dim E(\lambda_i)$ is odd;*

here $\overline{\lambda_i}(\chi),\ i = 1, 2$, are defined in (3.20).

Proof. By the argument of contradiction, we assume that (3.1) has no nonconstant positive solution. Then in the set $P_R \backslash \overline{P_r}$ there is only one fixed point, i.e., $\widetilde{\omega} = (u_c, \frac{\alpha}{\beta} u_c)$. Therefore, by Lemma 3.6, we have

$$\text{index}(\Psi, \widetilde{\omega}) = \text{index}(\Psi, P_R \backslash \overline{P_r})) = +1. \tag{3.27}$$

On the other hand, by Lemmas 3.7 and 3.9, we have

$$\text{index}(\Psi, \widetilde{\omega}) = \text{index}(\mathbb{J}, \widetilde{\omega}) = -1,$$

which contradicts (3.27). The proof is complete. ∎

Remark 3.1. It will be shown in section 5 that conditions (i) and (ii) are sufficient for generating a pattern solution which may not be stationary. Hence additional conditions are needed to warrant a stationary pattern solution. Theorem 3.10 says that items (iii) and (iv) will be such conditions.

Case study for $N = 1$. Consider system (3.1) with $N = 1$ and $\Omega = (0, l)$,

$$\begin{cases} -u'' + (\frac{\chi}{d_1} u(1-u)v')' = \frac{\mu}{d_1} u(1 - u/u_c), & x \in (0, l), \\ -v'' = \frac{\alpha}{d_2} u - \frac{\beta}{d_2} v, & x \in (0, l), \\ u'(0) = u'(l) = 0, \\ v'(0) = v'(l) = 0, \end{cases} \tag{3.28}$$

where $' = \frac{d}{dx}$. The eigenvalue problem associated with (3.28) is

$$\begin{cases} -\omega'' = \lambda \omega, \\ \omega'(0) = \omega'(l) = 0, \end{cases} \tag{3.29}$$

which has countably many eigenvalues $\lambda_i = \frac{(i-1)^2 \pi^2}{l^2},\ i = 1, 2, 3, \ldots$. Hence, by Theorem 3.10, we obtain the result on system (3.28).

PROPOSITION 3.11. *Assume that constants $d_1,\ d_2,\ \mu,\ \beta,\ \alpha,\ u_c$, and χ satisfy* (3.19) *and $\frac{\mu}{d_1} \neq \lambda_i = \frac{(i-1)^2 \pi^2}{l^2},\ i \geq 1$. If there exist integers $n_1,\ n_2$ satisfying $n_2 > n_1 \geq 1$ such that $\overline{\lambda_1}(\chi) \in (\lambda_{n_1}, \lambda_{n_1+1})$, $\overline{\lambda_2}(\chi) \in (\lambda_{n_2}, \lambda_{n_2+1})$ and $\sum_{i=n_1+1}^{n_2} \dim E(\lambda_i) = n_2 - n_1$ is odd, then system* (3.28) *has at least one nonconstant positive solution.*

Proof. Notice that when $\Omega = (0, l)$, the eigenvector corresponding to each eigenvalue λ_i is $\cos \frac{(i-1)\pi}{l} x$, which spans the eigenspace $E(\lambda_i)$. Hence $\dim E(\lambda_i) = 1$ and thus $\sum_{i=n_1+1}^{n_2} \dim E(\lambda_i) = n_2 - n_1$. Then the application of Theorem 3.10 completes the proof. ∎

4. Linear stability analysis for pattern formation. Mathematically, pattern formation is the process where a spatially homogeneous steady state becomes unstable, by varying a bifurcation parameter value, in the presence of spatially inhomogeneous perturbations, and a stable inhomogeneous solution arises. In this section, we shall employ linear stability analysis to identify the conditions for pattern formation of system (1.1)–(1.3) and compare them with conditions given in Theorem 3.10.

Let us first recall that system (1.1) without the chemotaxis term, namely system (2.2), has two homogeneous steady states $(0,0)$ and $(u_c, \frac{\alpha}{\beta}u_c)$. The former is unstable for (2.2) by simple calculations, and the latter is globally asymptotically stable for (2.2) as shown in Proposition 2.3. Hence we restrict our attention to finding the instability conditions for which $(u_c, \frac{\alpha}{\beta}u_c)$ becomes unstable in the presence of chemotaxis. The conventional method is to linearize (1.1) about $(u_c, \frac{\alpha}{\beta}u_c)$ and then look for solutions proportional to $e^{i\mathbf{k}\cdot\mathbf{x}+\sigma t}$, where $\mathbf{k}$ is the wave vector with magnitude $k = |\mathbf{k}|$ and σ is the temporal growth rate depending on k^2. Then patterns are expected when $\mathrm{Re}(\sigma) > 0$ for some $k > 0$ (see more details in [18]). Following this standard procedure, we can show that a necessary condition for the pattern formation of model (1.1) subject to homogeneous Neumann boundary conditions is

$$\chi > \chi_c = \frac{\mu d_2 + \beta d_1 + 2\sqrt{\mu\beta d_1 d_2}}{\alpha u_c(1-u_c)} \tag{4.1}$$

and that allowable wave number k satisfies

$$k_1^2 = \frac{-\eta - \sqrt{\eta^2 - 4d_1d_2\mu\beta}}{2d_1d_2} < k^2 < k_2^2 = \frac{-\eta + \sqrt{\eta^2 - 4d_1d_2\mu\beta}}{2d_1d_2}, \tag{4.2}$$

where $\eta = \mu d_2 + \beta d_1 - \chi\alpha u_c(1-u_c) < 0$. Condition (4.1) is necessary because allowable wave numbers are discrete in a finite domain, and hence the interval (k_1, k_2) does not necessarily contain the desired discrete number; for example, $k = \frac{n\pi}{l}$ for $n = 1, 2, \ldots$ if $\Omega = (0, l)$. The results derived in section 3 show that k^2 corresponds to the eigenvalue λ of the negative Laplace operator, namely, $\lambda = k^2$, $k_1^2 = \overline{\lambda_1}(\chi)$, $k_2^2 = \overline{\lambda_2}(\chi)$. Hence the instability of the homogeneous steady state $(u_c, \frac{\alpha}{\beta}u_c)$ occurs if (4.1) holds and

$$\text{there is a wave number } k \text{ such that (4.2) holds.} \tag{4.3}$$

Noticing that condition Theorem 3.10(i) is the same as (4.1) and Theorem 3.10(ii) is equivalent to (4.3), we have the following proposition.

PROPOSITION 4.1. *Let conditions Theorem* 3.10(i) *and* (ii) *hold. Then the homogeneous steady state* $(u_c, \frac{\alpha}{\beta}u_c)$ *of* (1.1)–(1.3) *is linearly unstable; namely, pattern formation of system* (1.1)–(1.3) *arises.*

It is helpful to note that conditions (4.1) and (4.3) (or Theorem 3.10(i) and (ii)) are not sufficient for ensuring that spatial patterns are stationary (see, e.g., Figure 3 in section 6), which is, however, warranted by two additional conditions Theorem 3.10(iii) and (iv). In this sense, conditions in Theorem 3.10(iii) and (iv) supplement the linear stability analysis results.

5. Bifurcation and stability analysis of patterns via the perturbation method. In this section, we apply the perturbation method to analyze the stationary pattern solutions with small amplitude, whose asymptotic expansions can be obtained via the standard bifurcation technique. By estimating the eigenvalue of the linearized system around the pattern solutions, we derive the stability/instability conditions

of stationary pattern solutions which provide a selection mechanism of the principal wave mode of the stable pattern. For simplicity, we restrict our attention to the one-dimensional case.

5.1. Bifurcation analysis. Considering the chemotaxis system (1.1)–(1.3) with $N = 1$ and $\Omega = (0, l)$, we have

$$\begin{cases} \dfrac{\partial u}{\partial t} = \dfrac{\partial}{\partial x}\left(d_1 \dfrac{\partial u}{\partial x} - \chi u(1-u)\dfrac{\partial v}{\partial x}\right) + \mu u(1-u/u_c), \quad x \in (0,l), \\ \dfrac{\partial v}{\partial t} = d_2 \dfrac{\partial^2 v}{\partial x^2} + \alpha u - \beta v, \quad x \in (0,l), \\ \dfrac{\partial u}{\partial x}\Big|_{x=0,l} = 0, \quad \dfrac{\partial v}{\partial x}\Big|_{x=0,l} = 0. \end{cases} \tag{5.1}$$

The steady states of (5.1) are the solutions to (3.28) in section 3. Obviously, $(u_c, \frac{\alpha}{\beta}u_c)$ is a positive constant solution of (3.28). Viewing χ as a bifurcation parameter, we now make an asymptotic analysis for the pattern solution (u^*, v^*) with small amplitude, which solves (3.28) and is bifurcated from $(u_c, \frac{\alpha}{\beta}u_c)$. Denote

$$g(u) = u(1-u), \qquad f(u) = u(1-u/u_c),$$

and assume

$$\begin{cases} u^* = u_c + \sum_{k=1}^{\infty} \varepsilon^k u_k = u_c + \varepsilon u_1 + \varepsilon^2 u_2 + \cdots + \varepsilon^k u_k + \cdots, \\ v^* = \frac{\alpha}{\beta}u_c + \sum_{k=1}^{\infty} \varepsilon^k v_k = \frac{\alpha}{\beta}u_c + \varepsilon v_1 + \varepsilon^2 v_2 + \cdots \varepsilon^k u_k + \cdots \end{cases} \tag{5.2}$$

and

$$\chi = \sum_{k=0}^{\infty} \varepsilon^k \chi_k = \chi_0 + \varepsilon\chi_1 + \varepsilon^2\chi_2 + \cdots + \varepsilon^k \chi_k + \cdots. \tag{5.3}$$

Here χ_0 is the possible bifurcation location of χ which will be found later. We now assume in (5.3) that the parameter χ is in the small neighborhood of the bifurcation location χ_0 so that the corresponding small amplitude solution (u^*, v^*) can be bifurcated at this location from the constant steady state $(u_c, \frac{\alpha}{\beta}u_c)$. We will see later that there are infinitely many bifurcation locations for χ_0 which can be denoted as $\chi_0(n),\ n = 1, 2, \ldots$.

Substituting (5.2) and (5.3) into (3.28) and equating the $O(\varepsilon)$ and $O(\varepsilon^2)$ terms, respectively, we get two systems

$$\begin{cases} d_1 u_1'' + \left(\frac{\chi_0 g(u_c)\alpha}{d_2} - \mu\right) u_1 - \frac{\chi_0 g(u_c)\beta}{d_2} v_1 = 0, \quad x \in (0,l), \\ d_2 v_1'' + \alpha u_1 - \beta v_1 = 0, \quad x \in (0,l), \\ u_1'(0) = u_1'(l) = 0, \\ v_1'(0) = v_1'(l) = 0 \end{cases} \tag{5.4}$$

and

$$\begin{cases} d_1 u_2'' + \left(\frac{\chi_0 g(u_c)\alpha}{d_2} - \mu\right) u_2 - \frac{\chi_0 g(u_c)\beta}{d_2} v_2 = F_1, \quad x \in (0,l), \\ d_2 v_2'' + \alpha u_2 - \beta v_2 = 0, \quad x \in (0,l), \\ u_2'(0) = u_2'(l) = 0, \\ v_2'(0) = v_2'(l) = 0, \end{cases} \tag{5.5}$$

where

$$F_1 = \chi_0 g'(u_c)u_1'v_1' + [\chi_0 g'(u_c)u_1 + \chi_1 g(u_c)]\, v_1'' - \frac{1}{2}\mu f''(u_c)u_1^2.$$

It is easy to get nonzero solutions (unique up to a constant multiple for any given positive integer n, and this constant can be absorbed into ε in (5.2)) for (5.4) as

$$\begin{cases} u_1 = c_1(n)\cos(\frac{n\pi}{l}x), \quad c_1(n) = \frac{\beta + d_2(\frac{n\pi}{l})^2}{\alpha}, \\ v_1 = \cos(\frac{n\pi}{l}x), \end{cases} \tag{5.6}$$

as long as χ_0 is given by

$$\chi_0 = \chi_0(n) = \frac{(d_1(\frac{n\pi}{l})^2 + \mu)(\beta + d_2(\frac{n\pi}{l})^2)}{\alpha u_c(1-u_c)(\frac{n\pi}{l})^2}, \qquad n = 1, 2, \ldots. \tag{5.7}$$

Here, to get the uniqueness of solution, we have assumed that for two given positive integers m and n,

$$\frac{(d_1(\frac{n\pi}{l})^2 + \mu)(\beta + d_2(\frac{n\pi}{l})^2)}{\alpha u_c(1-u_c)(\frac{n\pi}{l})^2} \neq \frac{(d_1(\frac{m\pi}{l})^2 + \mu)(\beta + d_2(\frac{m\pi}{l})^2)}{\alpha u_c(1-u_c)(\frac{m\pi}{l})^2} \quad \text{if} \quad m \neq n.$$

Mathematically, when χ is viewed as the bifurcation parameter, $\chi_0(n)$, $n = 1, 2, \ldots$, are called the possible bifurcation locations for the formation of new patterns. Denote

$$\chi_{\min} = \min_n \left\{ \frac{(d_1(\frac{n\pi}{l})^2 + \mu)(\beta + d_2(\frac{n\pi}{l})^2)}{\alpha u_c(1-u_c)(\frac{n\pi}{l})^2},\ n = 1, 2, \ldots \right\} = \chi_0(n_0)$$

for some positive integer n_0. Then it is easy to know that the first bifurcation occurs when the parameter χ crosses through the bifurcation value $\chi_{\min}$. If the bifurcation is stable, it will then yield patterns (u^*, v^*) with formulas given in (5.2) and (5.6).

To obtain the formula for χ_1, we first consider the adjoint system obtained from the left-hand side of (5.5):

$$\begin{cases} d_1 x_2'' + \left(\frac{\chi_0 g(u_c)\alpha}{d_2} - \mu\right) x_2 + \alpha y_2 = 0, \\ d_2 y_2'' - \frac{\chi_0 g(u_c)\beta}{d_2} x_2 - \beta y_2 = 0, \\ x_2'(0) = x_2'(l) = 0, \\ y_2'(0) = y_2'(l) = 0. \end{cases} \tag{5.8}$$

It is easy to compute that (5.8) has one solution

$$\begin{cases} x_2 = c_2(n)\cos(\frac{n\pi}{l}x), \quad c_2(n) = -\frac{\beta + d_2(\frac{n\pi}{l})^2}{\chi_0 g(u_c)\beta} d_2 < 0, \\ y_2 = \cos(\frac{n\pi}{l}x). \end{cases} \tag{5.9}$$

Multiplying the first equation of (5.5) by x_2 and the second by y_2, adding them together, and integrating the result in the interval $[0, l]$, we then obtain the solvability equation for χ_1. Direct computation gives

$$\chi_1 = \chi_1(n) = 0.$$

When $\chi_1 = 0$, for each n, F_1 in (5.5) can be simplified to

$$F_1 = -\frac{1}{4}\mu f''(u_c)c_1^2(n) - \left[\left(\frac{n\pi}{l}\right)^2 \chi_0 g'(u_c)c_1(n) + \frac{1}{4}\mu f''(u_c)c_1^2(n)\right]\cos\left(\frac{2n\pi}{l}x\right)$$

and a particular solution (u_2, v_2) of (5.5) can be found as

$$\begin{cases} u_2 = a_1(n) + a_2(n)\cos(\frac{2n\pi}{l}x), \\ v_2 = a_3(n) + a_4(n)\cos(\frac{2n\pi}{l}x), \end{cases} \tag{5.10}$$

where

$$\begin{aligned} a_1(n) &= \frac{1}{4}f''(u_c)c_1^2(n), \\ a_2(n) &= -\frac{(\beta + d_2(\frac{2n\pi}{l})^2)\left[(\frac{n\pi}{l})^2\chi_0 g'(u_c)c_1(n) + \frac{1}{4}\mu f''(u_c)c_1^2(n)\right]}{\alpha\chi_0 g(u_c)(\frac{2n\pi}{l})^2 - (d_1(\frac{2n\pi}{l})^2 + \mu)(\beta + d_2(\frac{2n\pi}{l})^2)}, \\ a_3(n) &= \frac{\alpha}{4\beta}f''(u_c)c_1^2(n), \\ a_4(n) &= -\frac{\alpha\left[(\frac{n\pi}{l})^2\chi_0 g'(u_c)c_1(n) + \frac{1}{4}\mu f''(u_c)c_1^2(n)\right]}{\alpha\chi_0 g(u_c)(\frac{2n\pi}{l})^2 - (d_1(\frac{2n\pi}{l})^2 + \mu)(\beta + d_2(\frac{2n\pi}{l})^2)}. \end{aligned} \tag{5.11}$$

Since $\chi_1 = 0$, for further analysis, we need to obtain χ_2. Following the process of getting (5.4) and (5.5), further computation up to the order $O(\varepsilon^3)$ gives

$$\begin{cases} d_1 u_3'' + \left(\frac{\chi_0 g(u_c)\alpha}{d_2} - \mu\right)u_3 - \frac{\chi_0 g(u_c)\beta}{d_2}v_3 = F_2, \\ d_2 v_3'' + \alpha u_3 - \beta v_3 = 0, \\ u_3'(0) = u_3'(l) = 0, \\ v_3'(0) = v_3'(l) = 0, \end{cases}$$

where the right-hand-side term F_2 is given by

$$\begin{aligned} F_2 = \chi_0 &\left[g'(u_c)(u_2v_1' + u_1v_2') + \frac{g''(u_c)}{2}u_1^2v_1'\right]' + \chi_2 g(u_c)v_1'' \\ &- \left[\mu f''(u_c)u_1u_2 + \mu\frac{f'''(u_c)}{3!}u_1^3\right], \end{aligned} \tag{5.12}$$

where $f'''(u_c) = 0$ can be directly calculated from the definition of the function f. The solvability condition can be simplified as

$$\int_0^l F_2\cos\left(\frac{n\pi}{l}x\right)dx = 0. \tag{5.13}$$

Substituting (5.12) into (5.13) yields

$$\begin{aligned} \chi_2(n) = &\frac{-2(\frac{n}{l}\pi)^2\chi_0\left[g'(u_c)(\frac{a_1(n)}{2} - \frac{1}{4}a_2(n) + \frac{c_1(n)a_4(n)}{2}) + \frac{g''(u_c)}{16}c_1^2(n)\right]}{g(u_c)(\frac{n\pi}{l})^2} \\ &- \frac{2\mu f''(u_c)c_1(n)\left(\frac{a_1(n)}{2} + \frac{a_2(n)}{4}\right)}{g(u_c)(\frac{n\pi}{l})^2}. \end{aligned} \tag{5.14}$$

In summary, we have now found all the bifurcation locations of χ as

$$\chi_0(n) = \frac{(d_1(\frac{n\pi}{l})^2 + \mu)(\beta + d_2(\frac{n\pi}{l})^2)}{\alpha u_c(1-u_c)(\frac{n\pi}{l})^2}, \qquad n = 1, 2, \ldots.$$

When the parameter χ given by (5.3) is in the neighborhood of $\chi_0(n)$ for each $n = 1, 2, \ldots$, the corresponding bifurcated solution (u^*, v^*) has a formula (5.2) with (u_1, v_1) and (u_2, v_2) given in (5.6) and (5.10), respectively.

To clarify the relationship between the solution (u^*, v^*) and its bifurcation location $\chi_0(n)$, we may relabel (u^*, v^*) as (u_n^*, v_n^*), i.e.,

$$\begin{cases} u_n^* = u_c + \varepsilon u_1 + \varepsilon^2 u_2 + \cdots, \\ v_n^* = \frac{\alpha}{\beta} u_c + \varepsilon v_1 + \varepsilon^2 v_2 + \cdots, \end{cases}$$

where (u_1, v_1) and (u_2, v_2) are n-dependent with formulas given in (5.6) and (5.10), respectively. We should mention that $(u_c, \frac{\alpha}{\beta} u_c)$ is called the *base* term of the pattern, and the pattern shape and its amplitude are determined primarily by the leading term (u_1, v_1) when ε is small. Note that this leading term happens to have the wave mode n; see (5.6). Therefore we also refer to n as the principal wave mode of the solution (u_n^*, v_n^*).

Remark 5.1. When the interval length l is sufficiently small, we have

(5.15)
$$\chi_0(n) = \frac{(d_1(\frac{n\pi}{l})^2 + \mu)(\beta + d_2(\frac{n\pi}{l})^2)}{\alpha u_c(1-u_c)(\frac{n\pi}{l})^2} \sim \frac{d_1 d_2}{\alpha u_c(1-u_c)} \left(\frac{n\pi}{l}\right)^2 \quad \text{for fixed } n = 1, 2, \ldots.$$

Then $\chi_0(n)$ attains minimal value when $n = n_0 = 1$. This means that the first bifurcation gives rise to a pattern with the principal wave mode $n_0 = 1$ when l is sufficiently small. Numerical simulations shown later in the paper also confirm this assertion. In the next subsection, we will show that the small amplitude steady states (u_n^*, v_n^*) are unstable if $n \neq n_0$, and it provides a selection mechanism of the principal wave mode for the volume-filling chemotaxis model.

Remark 5.2. We now give a relationship between $\chi_{\min}$ and χ_c. Since

$$\begin{aligned} \chi_{\min} = \chi_0(n_0) &= \frac{(d_1(\frac{n_0\pi}{l})^2 + \mu)(\beta + d_2(\frac{n_0\pi}{l})^2)}{\alpha u_c(1-u_c)(\frac{n_0\pi}{l})^2} \\ &= \frac{1}{\alpha u_c(1-u_c)} \left[d_1\beta + d_2\mu + d_1 d_2 \left(\frac{n_0\pi}{l}\right)^2 + \beta\mu \left(\frac{n_0\pi}{l}\right)^{-2} \right], \end{aligned}$$

it is easy to see that

$$\chi_{\min} \geq \frac{d_1\beta + \mu d_2 + 2\sqrt{d_1 d_2 \mu\beta}}{\alpha u_c(1-u_c)} = \chi_c,$$

where "=" holds if and only if

$$n_0 = \left(\frac{\mu\beta}{d_1 d_2}\right)^{\frac{1}{4}} \frac{l}{\pi} \tag{5.16}$$

is a positive integer and $\chi_0(n)$ attains its minimum at $n = n_0$. This means that the first bifurcation value $\chi_{\min}$ is usually greater than the critical value χ_c given in (3.19).

5.2. Stability analysis and selection mechanism. Now we are ready to find the stability of the pattern solution (u_n^*, v_n^*), bifurcated from the positive constant steady state, by estimating the sign of the principal eigenvalue.

For (5.1), set

$$\begin{cases} u = u_n^* + \phi e^{\lambda t}, \\ v = v_n^* + \varphi e^{\lambda t} \end{cases}$$

with

$$\begin{cases} \lambda = \lambda_0 + \varepsilon\lambda_1 + \varepsilon^2\lambda_2 + \cdots, \\ \phi = \phi_0 + \varepsilon\phi_1 + \cdots, \\ \varphi = \varphi_0 + \varepsilon\varphi_1 + \cdots \end{cases}$$

and

$$\begin{cases} u_n^* = u_c + \varepsilon u_1 + \varepsilon^2 u_2 + \cdots, \\ v_n^* = \frac{\alpha}{\beta} u_c + \varepsilon v_1 + \varepsilon^2 v_2 + \cdots, \\ \chi = \chi_0(n) + \varepsilon\chi_1(n) + \varepsilon^2\chi_2(n) + \cdots. \end{cases}$$

After substitution into (5.1), we first obtain a system by equating the $O(1)$ terms:

(5.17)
$$\begin{cases} d_1\phi_0'' + \left(\frac{\chi_0(n)g(u_c)\alpha}{d_2} - \mu\right)\phi_0 - \frac{\chi_0(n)g(u_c)\beta}{d_2}\varphi_0 = \lambda_0\phi_0 + \lambda_0\frac{\chi_0(n)g(u_c)}{d_2}\varphi_0, \quad x \in (0,l), \\ d_2\varphi_0'' + \alpha\phi_0 - \beta\varphi_0 = \lambda_0\varphi_0, \quad x \in (0,l), \\ \phi_0'(0) = \phi_0'(l) = 0, \\ \varphi_0'(0) = \varphi_0'(l) = 0. \end{cases}$$

The sign of λ_0 determines the stability of the stationary solution (u_n^*, v_n^*). To solve the eigenvalue problem (5.17), we can use (2.3) and (3.29) to replace (ϕ_0'', φ_0'') by $-(\frac{m\pi}{l})^2(\phi_0, \varphi_0)$ for some integer $m \geq 0$. The existence of nonzero solution (ϕ_0, φ_0) gives an equation for λ_0:

$$\lambda_0^2 + \left(d_1\left(\frac{m\pi}{l}\right)^2 + d_2\left(\frac{m\pi}{l}\right)^2 + \mu + \beta\right)\lambda_0 + C = 0, \tag{5.18}$$

where

$$C = \left(d_1\left(\frac{m\pi}{l}\right)^2 + \mu\right)\left(d_2\left(\frac{m\pi}{l}\right)^2 + \beta\right) - \chi_0(n)g(u_c)\alpha\left(\frac{m\pi}{l}\right)^2$$

and $\chi_0(n)$ is given by (5.7).

When $n \neq n_0$, we have $\chi_0 \neq \chi_{\min}$ and thus there exists an integer $m = n_0$ so that $C < 0$. As such, (5.18) has a positive root $\lambda_0 > 0$. Therefore, we have the following result, which gives a necessary condition for the stability of (u_n^*, v_n^*).

RESULT 5.1 (stability criterion). *When $n \neq n_0$, we have $\chi_0(n) \neq \chi_{\min}$ and the steady state (u_n^*, v_n^*) in (5.2) is unstable. In other words, if (u_n^*, v_n^*) is stable, then $n = n_0$.*

Next, when $n = n_0$, we have $\chi_0(n) = \chi_{\min}$. It is easy to know that the principal eigenvalue for (5.17) is $\lambda_0 = 0$ with eigenvector

$$(\phi_0, \varphi_0) = \left(\frac{\beta + d_2(\frac{n_0\pi}{l})^2}{\alpha}\cos\left(\frac{n_0\pi}{l}x\right), \cos\left(\frac{n_0\pi}{l}x\right)\right).$$

We then work on λ_1 and λ_2 to obtain the stability of $(u^*_{n_0}, v^*_{n_0})$. A further similar computation by equating the $O(\varepsilon)$ and $O(\varepsilon^2)$ terms, respectively, gives two systems:

(5.19)
$$\begin{cases} d_1\phi_1'' + \left(\frac{\chi_0(n_0)g(u_c)\alpha}{d_2} - \mu\right)\phi_1 - \frac{\chi_0(n_0)g(u_c)\beta}{d_2}\varphi_1 = \lambda_1\phi_0 + \lambda_1\frac{\chi_0(n_0)g(u_c)}{d_2}\varphi_0 + G_1, \\ d_2\varphi_1'' + \alpha\phi_1 - \beta\varphi_1 = \lambda_1\varphi_0, \\ \phi_1'(0) = \phi_1'(l) = 0, \\ \varphi_1'(0) = \varphi_1'(l) = 0 \end{cases}$$

and

(5.20)
$$\begin{cases} d_1\phi_2'' + \left(\frac{\chi_0(n_0)g(u_c)\alpha}{d_2} - \mu\right)\phi_2 - \frac{\chi_0(n_0)g(u_c)\beta}{d_2}\varphi_2 = \lambda_2\phi_0 + \lambda_2\frac{\chi_0(n_0)g(u_c)}{d_2}\varphi_0 + G_2, \\ d_2\varphi_2'' + \alpha\phi_2 - \beta\varphi_2 = \lambda_2\varphi_0, \\ \phi_1'(0) = \phi_1'(l) = 0, \\ \varphi_1'(0) = \varphi_1'(l) = 0, \end{cases}$$

where

$$G_1 = \chi_0(n_0)\left[g'(u_c)u_1\varphi_0'\right]' + \chi_0(n_0)\left[g'(u_c)v_1'\phi_0\right]' + \chi_1(n_0)g(u_c)\varphi_0'' - \mu f''(u_c)u_1\phi_0$$

and

$$\begin{aligned} G_2 = {} & \chi_0(n_0)g'(u_c)\left[v_1'\phi_1 + v_2'\phi_0 + u_1\varphi_1' + u_2\varphi_0'\right]' \\ & + \chi_0(n_0)g''(u_c)\left[u_1v_1'\phi_0 + \frac{1}{2}u_1^2\varphi_0'\right]' + \chi_2(n_0)g(u_c)\varphi_0'' \\ & - \mu f''(u_c)u_1\phi_1 - \mu\left[f''(u_c)u_2 + \frac{f'''(u_c)}{2}u_1^2\right]\phi_0. \end{aligned}$$

Thus, for (5.19), the solvability condition gives

$$\int_0^l \left(\lambda_1\phi_0 + \lambda_1\frac{\chi_0 g(u_c)}{d_2}\varphi_0 + G_1\right)x_2dx + \int_0^l \lambda_1\varphi_0 y_2dx = 0,$$

where (x_2, y_2) is given in (5.9) with $n = n_0$. Therefore, we have

$$\lambda_1 = \frac{-\int_0^l G_1x_2dx}{\int_0^l(\phi_0x_2 + \frac{\chi_0(n_0)g(u_c)}{d_2}\varphi_0x_2 + \varphi_0y_2)dx},$$

where

$$\begin{aligned} \int_0^l \left(\phi_0x_2 + \frac{\chi_0 g(u_c)}{d_2}\varphi_0x_2 + \varphi_0y_2\right)dx &= l\left(1 - \frac{\beta + d_2(\frac{n_0\pi}{l})^2}{\beta} - \frac{d_2(\beta + d_2(\frac{n_0\pi}{l})^2)^2}{\chi_0 g(u_c)\alpha\beta}\right) \\ &= -\frac{d_2(n_0\pi)^2 l}{\beta}\left(1 + \frac{\beta + d_2(\frac{n_0\pi}{l})^2}{\mu + d_1(\frac{n_0\pi}{l})^2}\right) < 0. \end{aligned} \tag{5.21}$$

A direct calculation yields

$$\int_0^l G_1x_2dx = 0$$

and hence

$$\lambda_1 = 0.$$

Now we need to compute λ_2. Since G_1 can be simplified as

$$\begin{aligned} G_1 = &-\frac{1}{2}\mu f''(\mu_c)c_1^2(n_0) \\ &-\left[2\Big(\frac{n_0\pi}{l}\Big)^2\chi_0(n_0)g'(u_c)c_1(n_0) + \frac{1}{2}\mu f''(\mu_c)c_1^2(n_0)\right]\cos\left(\frac{2n_0\pi}{l}x\right), \end{aligned}$$

with a straightforward computation, we have a particular solution (ϕ_1, φ_1) for (5.19) as

$$\begin{cases} \phi_1 = \bar{a}_1 + \bar{a}_2\cos(\frac{2n_0\pi}{l}x), \\ \varphi_1 = \bar{a}_3 + \bar{a}_4\cos(\frac{2n_0\pi}{l}x), \end{cases}$$

where

$$\bar{a}_i = 2a_i(n_0), \qquad n = 1, 2, 3, 4,$$

with a_1, a_2, a_3, a_4 defined in (5.11). Similarly, for (5.20), the solvability condition gives

$$\lambda_2 = \frac{-\int_0^l G_2 x_2 dx}{\int_0^l(\phi_0 x_2 + \frac{\chi_0 g(u_c)}{d_2}\varphi_0 x_2 + \varphi_0 y_2)dx}, \tag{5.22}$$

where

$$\begin{aligned} \int_0^l G_2 x_2 dx = lc_2\Big\{ &-\Big(\frac{n_0\pi}{l}\Big)^2\chi_0(n_0)g'(u_c)\left[\frac{3a_1}{2} - \frac{3a_2}{4} + \frac{3c_1a_4}{2}\right] \\ &-\frac{3}{16}\Big(\frac{n_0\pi}{l}\Big)^2\chi_0(n_0)g''(u_c)c_1^2 \\ &-\frac{1}{2}g(u_c)\Big(\frac{n_0\pi}{l}\Big)^2\chi_2(n_0) - \mu f''(u_c)c_1\left[\frac{3a_1}{2} + \frac{3a_2}{4}\right]\Big\}. \end{aligned}$$

The sign of λ_2 in (5.22) determines the stability of pattern $(u^*_{n_0}, v^*_{n_0})$. Since the denominator of (5.22) is negative (see (5.21)), the stability of the pattern solution $(u^*_{n_0}, v^*_{n_0})$ actually depends on the sign of numerator $\int_0^l G_2 x_2 dx$.

In the special case when $u_c = \frac{1}{2}$, then $g'(u_c) = 0$. Thus we have

$$I_0 = \int_0^l G_2 x_2 dx = lc_2c_1^3\left\{d_1\Big(\frac{n_0\pi}{l}\Big)^2 - 3\mu - \frac{2\mu^2[\beta + d_2(\frac{2n_0\pi}{l})^2]}{12d_1d_2(\frac{n_0\pi}{l})^4 - 3\mu\beta}\right\},$$

where (5.14) has been used. Thus we have the following result.

RESULT 5.2 (selection of principal wave modes). *Let $n_0 > 0$ be an integer at which $\chi_0(n)$ attains its minimum, namely, $\chi_{\min} = \chi_0(n_0)$. Then the small-amplitude steady state (u^*_n, v^*_n) is stable if $n = n_0$ and*

$$I = \int_0^l G_2 x_2 dx < 0.$$

Furthermore, if $u_c = \frac{1}{2}$*, then the small-amplitude steady state* (u_n^*, v_n^*) *is stable if and only if* $n = n_0$ *and* $I_0 < 0$ *(which is ensured if* μ *is small).*

Other than the bifurcation location χ_{n_0}, all the bifurcated stationary solutions (u_n^*, v_n^*) are unstable. The bifurcated pattern $(u_{n_0}^*, v_{n_0}^*)$ can be stable only at the location χ_{n_0}, and it happens to have n_0 as its principal wave mode in its asymptotic expansions. Therefore the two main results derived in this section explain the selection of principal wave modes of the small amplitude patterns in the evolution of the volume-filling chemotaxis model. Next we shall sketch part of the bifurcation branches. Assume $d_1 = 0.3,\ d_2 = 1,\ \mu = 0.5,\ \alpha = 10,\ \beta = 10,\ l = 10$, and $u_c = \frac{1}{2}$. It is easy to get

$$\chi_c = 2.3798 < \chi_{\min} = \chi_0(6) = 2.38926,$$

$$\chi_0(7) = 2.39389, \quad \chi_0(8) = 2.47461, \quad \chi_0(9) = 2.6095,$$

and

$$\chi_2(6) = -2.331, \quad \chi_2(7) = -0.705, \quad \chi_2(8) = 0.709, \ \chi_2(9) = 2.334.$$

As such, the indication of four bifurcation branches when χ nears four locations $\chi_0(n),\ n = 6, 7, 8$, and 9, is drawn in Figure 1. It is worthwhile to mention that the first bifurcation at $\chi_0(6)$ is backwards and such a kind of bifurcation was also previously found in [26] for the volume-filling chemotaxis model (1.1) without cell growth (i.e., $\mu = 0$).

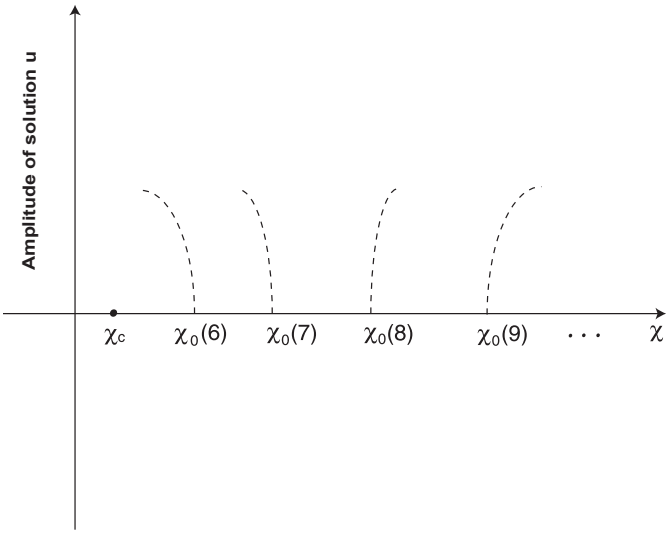

FIG. 1. *Bifurcation diagram:* $\chi_{\min} = \chi_0(6)$*. The solid branch means a stable pattern, and the dotted branches mean unstable pattern solutions.*

5.3. Steady state with large amplitude. We finally make a remark about the existence of a nonconstant steady state with large amplitude.

We assume the existence of this type of steady state in a long interval $[0, k]$. Set

$$x = ky.$$

After this scaling, system (3.28) reads as

$$\begin{cases} 0 = d_1 \frac{1}{k^2}\frac{d^2u}{dy^2} - \frac{\chi}{k^2}\frac{d}{dy}\left(u(1-u)\frac{dv}{dy}\right) + \mu u(1-u/u_c), \quad y \in (0,1), \\ 0 = d_2 \frac{1}{k^2}\frac{d^2v}{dy^2} + \alpha u - \beta v, \quad y \in (0,1), \\ u'(0) = u'(1) = 0, \\ v'(0) = v'(1) = 0. \end{cases}$$

When k is large and $\chi = O(k^2)$, the leading term equation of (u, v) is given by

$$\begin{cases} 0 = -\frac{\chi}{k^2}\frac{d}{dy}\left(u(1-u)\frac{dv}{dy}\right) + \mu u(1-u/u_c), \\ 0 = \alpha u - \beta v, \\ u'(0) = u'(1) = 0, \\ v'(0) = v'(1) = 0 \end{cases}$$

or

$$\begin{cases} 0 = -\frac{\chi}{k^2}\left(\frac{\alpha}{\beta}u(1-u)u'\right)' + \mu u(1-u/u_c), \\ u'(0) = u'(1) = 0. \end{cases} \tag{5.23}$$

Let

$$W = \int_0^u s(1-s)ds = \frac{u^2}{2} - \frac{u^3}{3}, \qquad W_c = \frac{u_c^2}{2} - \frac{u_c^3}{3}. \tag{5.24}$$

When u is in the interval $[0, 1]$, $W(u)$ is an increasing function and this defines an inverse function $u(W)$. From (5.24), we get

$$W'(x) = u(1-u)u'$$

and system (5.23) becomes

$$\begin{cases} W'' - \frac{\mu k^2 \beta}{\chi \alpha} u(W)\left(1 - \frac{u(W)}{u_c}\right) = 0, \\ W'(0) = W'(1) = 0. \end{cases} \tag{5.25}$$

Set $Q(W) = \frac{\mu k^2 \beta}{\chi \alpha} u(W)(1 - \frac{u(W)}{u_c})$. We have $Q(0) = Q(W_c) = 0$, $Q(x) > 0$ for $x \in (0, W_c)$, and

$$Q(W) \sim \sqrt{2}\sqrt{W} \quad \text{as} \quad W \to 0.$$

A standard phase plane analysis on equation

$$W'' - Q(W) = 0$$

can give rise to solutions with large amplitudes to (5.25). Once we have the solution W, the inverse transform $u(W)$ can give the solution u, which also has large amplitude. This explains the existence of stationary solution (u, v) with large amplitude. Since the formula of this solution is unknown, theoretical analysis of the stability of this solution is still a challenging problem which has to be left open.

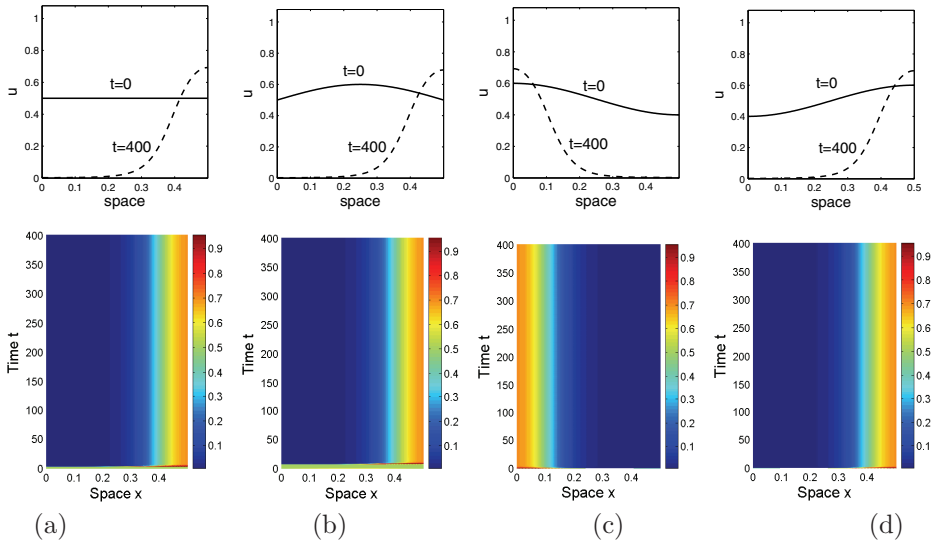

FIG. 2. *Pattern formation of the volume-filling model* (1.1)–(1.3) *in a one-dimensional small domain* $\Omega = (0, 0.5)$ *for different initial data which are small perturbations of the spatially homogeneous steady state* $(u_c, \frac{\alpha}{\beta}u_c)$*, where parameter values are* $d_1 = 0.1,\ d_2 = 1,\ \mu = 1,\ u_c = 0.5,\ \alpha = 1,\ \beta = 1,\ \chi = 50$*. The respective initial conditions are* (a) $u_0 = 0.5,\ v_0 = 0.6$*;* (b) $u_0 = v_0 = 0.5 + 0.1\cos(2\pi(0.25 - x))$*;* (c) $u_0 = v_0 = 0.5 + 0.1\cos(2\pi x)$*;* (d) $u_0 = v_0 = 0.5 + 0.1\cos(2\pi(x - 0.5))$.

6. Numerical simulation of spatial patterns. In this section, we show the numerical simulations of model (1.1)–(1.3) in one- and two-dimensional spaces to illustrate our theoretical results and demonstrate the patterns generated by the system. In Figure 2, we simulate the full nonlinear model (1.1)–(1.3) in a small domain for different initial conditions, where we obtain the stationary spatial patterns with cell aggregates at the boundary. There exist two spatial patterns $u_1(x)$ and $u_2(x)$ which are symmetrical in the relation $u_2(x) = u_1(l - x)$ (see Figure 2(c), (d)), a fact that can be seen from (3.28) directly. As shown in section 5, the unstable wave numbers are discrete values $k = \frac{n\pi}{l}$, $n = 1, 2, \ldots$, where the wave mode n, which corresponds to the spatial mode function $\cos(\frac{n\pi x}{l})$, determines the number of aggregates and satisfies $k_1 < \frac{n\pi}{l} < k_2$. A simple calculation based on the parameter values given in Figure 2 yields $k_1 = 0.2963,\ k_2 = 10.673$. So the wave mode when $l = 0.5$ is $n = 1$, which corresponds to a single boundary aggregate, as shown in Figure 2. Moreover, since the domain is small so that $n = 1$ corresponds to the first bifurcation location of the chemotactic coefficient (see Remark 5.1), the stationary patterns are stable by Result 5.2, which is exactly confirmed by our numerical simulations. In this simulation, we should also mention that when the domain size is small, the first location of a bifurcation parameter becomes large (see (5.15)) so that $\chi_{\min} = \chi_0(1) = 20.3$ and $\chi_0(2) = 67.60$. Our choice $\chi = 50$ is between these values. In Figure 3, we increase the domain length and find that patterns may change dramatically when the parameter χ is far away from the first bifurcation value $\chi_{\min}$. There are several findings in Figure 3: (1) The number of cell aggregations increases as the domain length increases. (2) When the domain is large, there is a persistent patterning process of merging (two neighboring aggregates join to form a new single aggregate with a larger interval of low cell density) and emerging (a new aggregate develops from a region of low cell density). Such a patterning process is called "coarsening process" in [22].

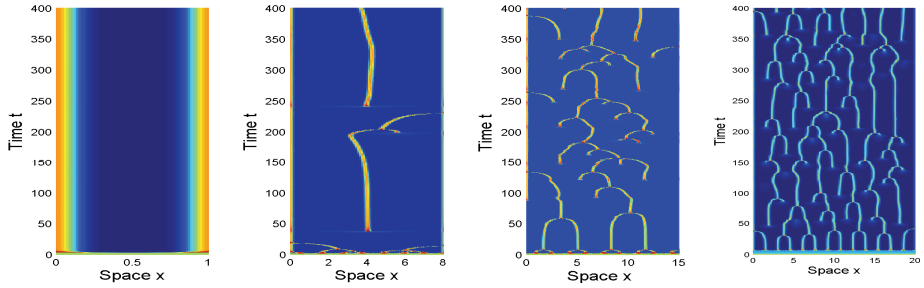

FIG. 3. *Pattern formation of the volume-filling model* (1.1)–(1.3) *in one-dimensional domains of different lengths, where initial conditions* $u_0 = 0.5$, $v_0 = 0.6$ *are taken to be a small uniform perturbation of the spatially homogeneous steady state and parameter values are* $d_1 = 0.1$, $d_2 = 1$, $\mu = 1$, $u_c = 0.5$, $\alpha = 1$, $\beta = 1$, $\chi = 50$.

For a small domain, there is no coarsening process. A similar patterning behavior regarding the domain size has been numerically demonstrated in a recent paper by Painter and Hillen [23] for a chemotaxis model without a volume-filling effect. For fixed parameter values, the wave numbers k_1 and k_2 are fixed and the unstable wave modes n satisfy

$$\frac{k_1 l}{\pi} < n < \frac{k_2 l}{\pi}. \tag{6.1}$$

Clearly the range of modes n increases with respect to the domain length l. Hence more unstable modes (i.e., aggregates) arise as the domain is elongated. Eventually the unstable spatial modes overlap and the interaction of unstable spatial modes leads to irregular spatial patterns. This indicates that the complex spatial patterns arise only if the domain length is large in the case when other parameters are fixed, as shown by the sequential simulations in Figure 3. It is worthwhile to point out that the critical domain length of emerging patterns was studied by Painter and Hillen [23].

Figure 3 shows that the spatial patterns become intricate and tend to be unstable as the domain length increases when χ is far away from $\chi_{\min}$. Typically the dynamics exhibits a chaotic behavior of alternating merging and emerging processes; see the last two pictures of Figure 3. However, if we choose the parameter χ close to the first bifurcation location $\chi_{\min}$, the evolution of patterns appears to be stationary; see Figure 4(a). When the parameter χ is close (or mildly close) to the first bifurcation value $\chi_{\min}$, the stationary wave amplitudes are small due to weak chemotactic strength. Using the parameter values for numerical simulation in Figure 4, we can calculate that when $n_0 = 13$, χ_0 obtains its minimum value $\chi_0(n_0) = 2.3800$, which is greater than the critical number $\chi_c = 2.3798$. Since the profiles of stationary pattern solutions are approximated by (5.2) and (5.6), there are six peaks (boundary peak counts as a half peak) and six wells, as shown in Figure 4(c). Hence there will be six visible stable peaks (or aggregates), as shown in Figure 4(a). The simulation in Figure 4(a) is also consistent with our main results in Theorem 3.10. Indeed, by the parameter values chosen in Figure 4(a), we have that $5 = \chi > \chi_c = 2.3798$, which satisfies condition (i) of Theorem 3.10. Furthermore, according to the formulas in (3.20), we have $\overline{\lambda_1}(\chi) = 0.7525$ and $\overline{\lambda_2}(\chi) = 5.4253$. It is easy to verify that we can find $15 = n > n_1 = 6$ such that $\overline{\lambda_1}(\chi) \in (\lambda_6, \lambda_7)$ and

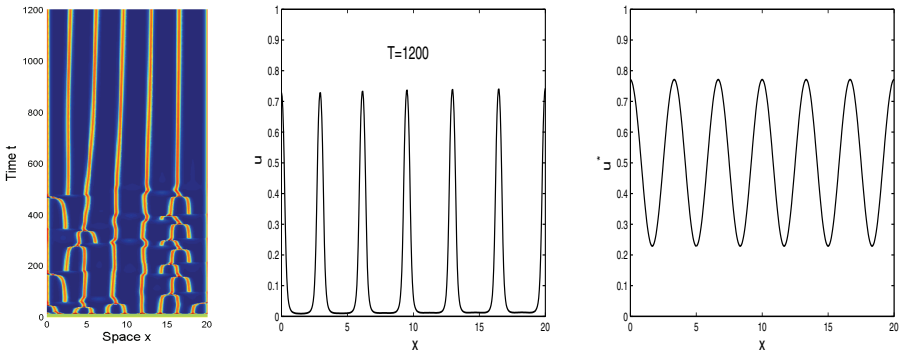

(a) (b) (c)

FIG. 4. *Stationary patterns of the volume-filling model* (1.1)–(1.3) *for large domain* $\Omega = (0, 20)$, *where initial data* $u_0 = v_0 = 0.6$ *and parameter values are chosen as follows:* $d_1 = 0.3$, $d_2 = 1$, $\mu = 0.5$, $u_c = 0.5$, $\alpha = 10$, $\beta = 10$, $\chi = 5$.

$\overline{\lambda_2}(\chi) \in (\lambda_{15}, \lambda_{16})$. Hence condition (ii) of Theorem 3.10 is fulfilled. By calculating $\frac{\mu l^2}{d_1 \pi^2} = 67.5475$, which is not an integer, condition (iii) of Theorem 3.10 is satisfied. Finally $\sum_{i=n_1+1}^{n} \dim E(\lambda_i) = n - n_1 = 15 - 6 = 9$ is odd, which verifies condition (iv) of Theorem 3.10. Hence, by Theorem 3.10, there exists a nonconstant stationary solution (or pattern) as given in Figure 4(a). Moreover, Figure 4(b) plots the stable solution profile u shown in Figure 4(a) to compare with the analytical approximate pattern in Figure 4(c), where there exist some variations in shape since the simulation in Figure 4(c) ignores the higher order terms. However, the number of stable aggregates, which is the most interesting component, is precisely predicted by Result 5.2.

Next we explore the numerical spatial patterns in two-dimensional domains. Figure 5 shows the spatio-temporal pattern at different time steps in a small domain $\Omega = (0, 2) \times (0, 2)$, which exhibits a patterning process similar to the one-dimensional case. The stationary aggregations eventually locate on the boundary, precisely on the part of the boundary with the largest curvature (i.e., the corners of the rectangle). There is no coarsening process occurring for the small domain. Similar to the one-dimensional case, the pattern becomes intricate as the domain size increases, as shown in Figure 6, where we simulate the model in a two-dimensional large domain $\Omega = (0, 20) \times (0, 20)$ and observe the complex merging and emerging processes of pattern formation.

Finally we remark that the stationary solution amplitudes shown in the above numerical simulations might not be small enough to comply with the requirement for the linear stability analysis given in section 5. In this case, the numerical simulations are indeed beyond our analytical results and may make predictions for the large amplitude stationary solutions for which nonlinear stability analysis is needed to determine the stability criteria.

7. Summary and discussion. In this paper, we derive the sufficient conditions for the existence of stationary solutions of a volume-filling chemotaxis model with logistic growth under zero flux boundary conditions; see Theorem 3.10. The partial conditions of Theorem 3.10 coincide with the conditions of pattern formations derived by the linear stability analysis given in section 4; see also Proposition 4.1. By

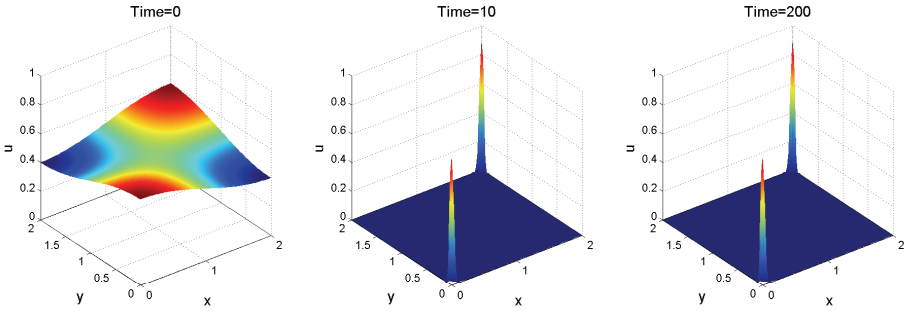

FIG. 5. *Stationary spatial patterns of the volume-filling model* (1.1)–(1.3) *on a two-dimensional small domain* $\Omega = (0,2)\times(0,2)$*, where parameter values are* $d_1 = 0.1$, $d_2 = 1$, $\mu = 1$, $u_c = 0.5$, $\alpha = 1$, $\beta = 1$, $\chi = 50$. *The initial conditions are set as a small perturbation of the homogeneous steady state, where* $u_0 = v_0 = 0.5 + 0.1\cos(\pi x/2)\cos(\pi y/2)$.

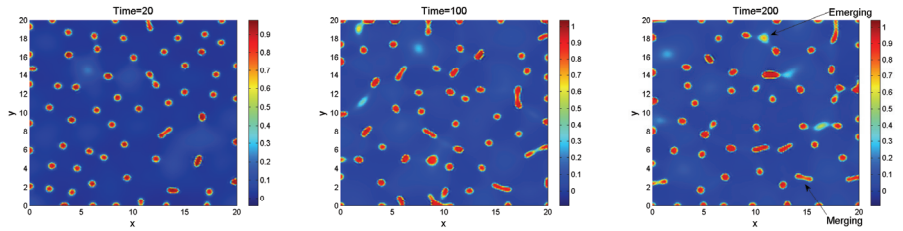

FIG. 6. *Pattern formation of the volume-filling model* (1.1)–(1.3) *on a two-dimensional large domain* $\Omega = (0,20)\times(0,20)$*, where parameter values are* $d_1 = 0.1$, $d_2 = 1$, $\mu = 1$, $u_c = 0.5$, $\alpha = 1$, $\beta = 1$, $\chi = 20$. *The initial conditions are* $u_0 = 0.5$, $v_0 = 0.6$. *The red dots (or, rods) mean the aggregation of cells where cell density is higher than the blue area; see the color bar. Color is available only in the online version.*

bifurcation analysis, we find the approximate stationary pattern solutions with small amplitudes and identify the stability/instability conditions for them. The numerical simulations are performed, which explain some of our analytical results and exhibit a variety of interesting patterns. Strikingly, for the dynamical evolution of solutions to stationary patterns, we employ asymptotic analysis to find a necessary stability condition (see Result 5.1) and provide a selection mechanism of the principal wave modes for stable stationary patterns (see Result 5.2). Precisely speaking, if the stationary pattern solution is stable, then its principal wave mode n must be a positive integer n_0 at which the quantity

$$\chi_0(n) = \frac{(d_1(\frac{n\pi}{l})^2 + \mu)(\beta + d_2(\frac{n\pi}{l})^2)}{\alpha u_c(1-u_c)(\frac{n\pi}{l})^2}, \qquad n = 1, 2, \ldots,$$

is minimized. These results provide an easy way to predict the solution profile and manage to explain the occurrence of stationary patterns and the number of aggregates in our numerical simulations as long as the parameter χ is close to the first bifurcation value $\chi_{\min}$. We want to point out that our methods and results exhibited in the paper work not only for the volume-filling chemotaxis model but also for a class of chemotaxis models with cell growth in which the chemosensitivity function depends on the cell density.

There are various interesting questions arising from our present analytical and numerical studies. Noticing that Theorem 3.10 is derived based on the degree index

theory, it is unclear whether or not sufficient conditions in Theorem 3.10 can be relaxed by other approaches. Moreover, when the domain length is large and the parameter values are far from the first bifurcation location, the patterns exhibit a kind of chaotic dynamics (see, e.g., Figure 3) whose mathematical mechanism is not well understood yet. While the mechanism of the emerging process in the pattern formation was identified in [23], the mathematical understanding of the merging process still remains open. All these questions, related to global bifurcation and stability analysis, are very interesting and worthwhile to pursue in the future.

Acknowledgments. The authors would like to thank the referees for their valuable comments, which greatly improved the exposition of the paper. The second author would like to thank the Department of Mathematics at the City University of Hong Kong for its hospitality and the help of its members during his stay there while on his sabbatical leave.

REFERENCES

[1] H. Amann, *Fixed point equations and nonlinear eigenvalue problems in ordered Banach spaces*, SIAM Rev., 18 (1976), pp. 620–709.

[2] H. Amann, *Nonhomogeneous linear and quasilinear elliptic and parabolic boundary value problems*, in Function Spaces, Differential Operators, and Nonlinear Analysis, Teubner-Texte Math. 133, Teubner, Stuttgart, 1993, pp. 9–126.

[3] E. Budrene and H. Berg, *Complex patterns formed by motile cells of Escherichia coli*, Nature, 349 (1991), pp. 630–633.

[4] E. Budrene and H. Berg, *Dynamics of formation of symmetrical patterns by chemotactic bacteria*, Nature, 376 (1995), pp. 49–53.

[5] Y. Du, P. Y. H. Pang, and M. Wang, *Qualitative analysis of a prey-predator model with stage structure for the predator*, SIAM J. Appl. Math., 69 (2008), pp. 596–620.

[6] L. Dung and H. L. Smith, *Steady states of models of microbial growth and competition with chemotaxis*, J. Math. Anal. Appl., 229 (1999), pp. 295–318.

[7] R. M. Ford and D. A. Lauffenburger, *Measurement of bacterial random motility and chemotaxis coefficients:* II. *Application of single cell based mathematical model*, Biotechnol. Bioeng., 37 (1991), pp. 661–672.

[8] R. M. Ford, B. R. Phillips, J. A. Quinn, and D. A. Lauffenburger, *Measurement of bacterial random motility and chemotaxis coefficients:* I. *Stopped-flow diffusion chamber assay*, Biotechnol. Bioeng., 37 (1991), pp. 647–660.

[9] D. Gilbarg and N. S. Trudinger, *Elliptic Partial Differential Equations of Second Order*, Springer, Berlin, 1977.

[10] T. Hillen and K. Painter, *A user's guide to PDE models for chemotaxis*, J. Math. Biol., 57 (2009), pp. 183–217.

[11] T Höfer, J. A. Sherratt, and P. K. Maini, *Dictyostelium discoideum: Cellular self-aggregation in an excitable medium*, Proc. R. Soc. Lond. B, 259 (1995), pp. 249–257.

[12] D. Horstmann, *From* 1970 *until present: The Keller-Segel model in chemotaxis and its consequences* I, Jahresber. Deutsch. Math.-Verein., 105 (2003), pp. 103–165.

[13] J. Jiang and Y. Y. Zhang, *On convergence to equilibria for a chemotaxis model with volume-filling effect*, Asymptot. Anal., 65 (2009), pp. 79–102.

[14] E. F. Keller and L. A. Segel, *Initiation of slime mold aggregation viewed as an instability*, J. Theoret. Biol., 26 (1970), pp. 399–415.

[15] E. F. Keller and L. A. Segel, *Model for chemotaxis*, J. Theoret. Biol., 30 (1971), pp. 225–234.

[16] P. Laurencot and D. Wrzosek, *A chemotaxis model with threshold density and degenerate diffusion*, in Nonlinear Elliptic and Parabolic Problems, Progr. Nonlinear Differential Equations Appl. 64, Birkhäuser, Basel, 2005, pp. 273–290.

[17] S. G. Li and K. Muneoka, *Cell migration and chick limb development: Chemotactic action of FGF-4 and the AER*, Dev. Cell, 211 (1999), pp. 335–347.

[18] J. D. Murray, *Mathematical Biology* II: *Spatial Models and Biomedical Applications*, 3rd ed., Springer, Berlin, 2002.

[19] L. Nirenberg, *Topics in Nonlinear Functional Analysis*, American Mathematical Society, Providence, RI, 2001.

[20] K. Osaki, T. Tsujikawa, A. Yagi, and M. Mimura, *Exponential attractor for a chemotaxis-growth system of equations*, Nonlinear Anal., 51 (2002), pp. 119–144.
[21] C. Ou and W. Yuan, *Traveling wavefronts in a volume-filling chemotaxis model*, SIAM J. Appl. Dyn. Syst., 8 (2009), pp. 390–416.
[22] K. Painter and T. Hillen, *Volume-filling and quorum-sensing in models for chemosensitive movement*, Can. Appl. Math. Q., 10 (2002), pp. 501–543.
[23] K. J. Painter and T. Hillen, *Spatio-temporal chaos in a chemotaxis model*, Phys. D, 240 (2011), pp. 363–375.
[24] K. J. Painter, P. K. Maini, and H. G. Othmer, *Stripe formation in juvenile pomacanthus explained by a generalized Turing mechanism with chemotaxis*, Proc. Natl. Acad. Sci. USA, 96 (1999), pp. 5549–5554.
[25] K. J. Painter, P. K. Maini, and H. G. Othmer, *A chemotactic model for the advance and retreat of the primitive streak in avian development*, Bull. Math. Biol., 62 (2000), pp. 501–525.
[26] A. Potapov and T. Hillen, *Metastability in chemotaxis models*, J. Dynam. Differential Equations, 17 (2005), pp. 293–330.
[27] H. L. Smith, *Monotone Dynamical Systems: An Introduction to the Theory of Competitive and Cooperative Systems*, Math. Surveys Monogr. 41, American Mathematical Society, Providence, RI, 1995.
[28] J. I. Tello and M. Winkler, *A chemotaxis system with logistic source*, Comm. Partial Differential Equations, 32 (2007), pp. 849–877.
[29] A. M. Turing, *The chemical basis of morphogenesis*, Phil. Trans. Roy. Soc. B, 237 (1952), pp. 5–72.
[30] Z. A. Wang and T. Hillen, *Classical solutions and pattern formation for a volume filling chemotaxis model*, Chaos, 17 (2007), 037108.
[31] M. Winkler, *Boundedness in the higher-dimensional parabolic-parabolic chemotaxis system with logistic source*, Comm. Partial Differential Equations, 35 (2010), pp. 1516–1537.
[32] D. Wrzosek, *Global attractor for a chemotaxis model with prevention of overcrowding*, Nonlinear Anal., 59 (2004), pp. 1293–1310.
[33] D. Wrzosek, *Long time behaviour of solutions to a chemotaxis model with volume filling effect*, Proc. Roy. Soc. Edinburgh Sect. A, 136 (2006), pp. 431–444.
[34] X. S. Yang, D. Dormann, A. E. Munsterberg, and C. J. Weijer, *Cell movement patterns during gastrulation in the chick are controlled by positive and negative chemotaxis mediated by FGF4 and FGF8*, Dev. Cell, 3 (2002), pp. 425–437.